INVESTIGATING THE IMPACT OF ENVIRONMENTAL CONDITIONS ON METAL-MICROBE DYNAMICS IN WETLANDS

by

MARILEE C. HOYLE

(Under the Direction of Raven Bier)

ABSTRACT

Wetlands are vital ecosystems vulnerable to threats including metal contamination. Microorganisms can mediate metal fate and bioavailability, but the influence of environmental factors—particularly light exposure—on these interactions remains unclear. Previous works have shown that light can influence these communities, however its consequences for metal dynamics is understudied. We conducted a microcosm experiment using two wetlands—a constructed site and a natural depressional wetland at the Savannah River Site (Aiken, SC). Microbial communities were incubated under light and dark conditions, with copper added at the midway point. We assessed how light influenced microbial-driven copper transport and distribution between sediment and water. Our findings show that light significantly alters microbial community alpha diversity and membership, promoting copper retention in sediments under ambient conditions but lessening it under elevated copper stress. These results highlight abiotic factors like light shape microbial processes, informing strategies for wetland conservation and metal contamination management.

INDEX WORDS: Microbial communities, Wetlands, Metal contamination, Management

INVESTIGATING THE IMPACT OF ENVIRONMENTAL CONDITIONS ON METAL-MICROBE DYNAMICS IN WETLANDS

by

MARILEE C. HOYLE

B.S., Oregon State University, 2020

A Thesis, Submitted to the Graduate Faculty of The University of Georgia in Partial Fulfillment of the Requirements for the Degree

MASTER OF SCIENCE

ATHENS, GEORGIA

2025

INVESTIGATING THE IMPACT OF ENVIRONMENTAL CONDITIONS ON METAL-MICROBE DYNAMICS IN WETLANDS

by

MARILEE C. HOYLE

Major Professor:	Raven L. Bier
Committee:	Xiaoyu Xu
	Alexander Strauss

Electronic Version Approved:

Ron Walcott
Vice Provost for Graduate Education and Dean of the Graduate School
The University of Georgia
August 2025

DEDICATION

I dedicate this work to my family—Laura Hoyle, Ken Hoyle, Emailee Hoyle, Jessica Cazares, and Francisco Cazares. Thank you for your love, support, and all the sacrifices you've made. I would not be here without you.

ACKNOWLEDGEMENTS

I want to thank everyone who has supported me throughout my academic journey. I am especially grateful to my committee members—Dr. Raven Bier, Dr. Alexander Strauss, and Dr. Xiaoyu Xu—for their guidance, insight, and encouragement.

Thank you to my lab mates and friends for your support and camaraderie during this process. Your presence made even the most challenging days manageable.

And finally, thank you to my cat Wibbles for being a source of comfort and comic relief during stressful moments. Your presence brought me peace and reminded me to pause and breathe.

TABLE OF CONTENTS

Page

APPENDICES

LIST OF TABLES

LIST OF FIGURES

CHAPTER 1

INTRODUCTION

Wetlands are one of the many ecosystems on Earth where microorganisms play essential roles for their function (Balkcom et al., 2000). Wetlands are critical aquatic ecosystems, which host diverse water-tolerant species and provide essential services such as flood control, climate regulation, and nutrient cycling (Balkcom et al., 2000). In these systems, microbial communities regulate nutrient availability, decompose organic material, and mediate the redox transformation of elements, including metals that can pose contamination risks. Wetlands are increasingly threatened by both habitat loss and contamination, with a 33% global loss recorded as of 2009, signifying a sharp decline in critical ecosystem function (Hu et al., 2017).

One of the key stressors to wetlands is climate change, which is already altering environmental conditions that affect many of Earth's ecosystems. Recent evidence indicated that along with consequences to precipitation and temperature patterns, climate change is driving decreases in cloud cover over the southeast of North America due to shifts in storm tracks and expansion of dry zones (Norris et al., 2016). Because clouds regulate the amount of solar radiation reaching the Earth's surface, these decreases can increase light intensity. Such changes in light have the potential to alter microbial activity and biogeochemical cycling in wetlands.

Another important stressor to wetlands is excessive metal contaminants from aerial deposition, industrial runoff, or other sources can include pollutants such as copper, zinc, and lead which can disrupt or enhance microbial processes and negatively impact macrofauna by interfering with immune and reproductive systems (Richard et al., 2021; Wilson et al., 2007).

Copper is one of the most frequently detected metal pollutants in environments influenced by human activities, often occurring alongside metals like zinc and lead (Franson et al., 2012; Rahimzadeh et al., 2024). Copper is an essential trace element vital for many biological processes, including enzyme function, immune response, and energy production (Trevors & Cotter, 1990; Rensing & Grass, 2003; Ladomersky & Petris, 2015). Despite these benefits, elevated copper concentrations in water have been linked to serious health issues in wildlife, including anemia, convulsions, and coma, while in migratory birds, copper exposure has been associated with decreased reproductive success, neurotoxicity, and mortality (Franson, Lahner, Meteyer, & Rattner, 2012; Rahimzadeh et al., 2024). Regarding microbiota effects, extreme copper concentrations are toxic to microalgae by impairing photosynthesis and growth, but some microalgae show potential for copper bioremediation (Cavalletti et al. 2022). Despite these threats and the potential for microbially-based bioremediation, our understanding of how microbial communities influence the bioavailability of metals in wetland ecosystems remains incomplete.

Copper has two main pathways of precipitation from the water column: oxidative reactions take place in rich oxygen environments, promoting the binding of metals to humic substances or iron oxides, while reductive processes take place mostly in oxygen poor locations and are driven by microbial activity leading to the formation of compounds like copper sulfides. Both pathways contribute to metal precipitation and accumulation in sediments (Eger, 1994; Christensen et al., 2000). However, metals bound under oxidative conditions tend to be more mobile and bioavailable compared to the more stable, less soluble metal forms produced under reducing conditions (Kang et al., 2019).

Multiple factors interact with microbial activity in wetlands to influence metal fate, including nutrients, seasons, oxygen, and light availability, which collectively shape whether reductive or oxidative processes dominate. For example, orthophosphate in the water column can interact with copper by forming insoluble copper-phosphate precipitates, reducing dissolved copper concentrations and bioavailability (Lytle, Schock, Leo, & Barnes, 2018). Seasonality plays a key role, as the time of year impacts plant growth, organic matter inputs, and oxygen dynamics (Xu and Mills, 2018). During late summer in North America's Southeast reason region, increased wetland plant growth combined with lower oxygen concentrations promotes the activity of sulfate-reducing prokaryotes (SRPs). This environment favors reductive processes that lead to the formation and immobilization of metals such as copper sulfide particulates, which accumulate in sediments (Xu and Mills, 2018). In contrast, during winter, sulfur-oxidizing prokaryotes (SOPs) utilize available oxygen and hydrogen sulfide (H_2S) for energy, reducing sulfide availability for metal precipitation (Eger, 1994; Christensen et al., 2000). Increased oxygen during this period enhances oxidative processes, promoting the formation of metal oxides or metal binding to humic substances and iron oxides, ultimately leading to metal deposition in sediments in forms that are easily remobilized to the water column (Xu and Mills, 2018).

Decomposition, through complex microbial interactions, has the potential to facilitate the production and presence of metal-organic complexes (Rosemond et al., 2015), which are more bioavailable than metal sulfides. Additionally, increased light can stimulate photosynthetic carbon fixation, producing organic matter that accumulates as floc. As this material decomposes, microbial chelation processes may further influence the cycling and speciation of metals

(Rosemond et al., 2015). The influence from oxygen and light availability on the dominance of oxidation or reduction reactions is integrated by the activity of photosynthetic microorganisms.

Under restricted light conditions, oxygen production by photoautotrophs declines, which may limit the activity of sulfur-oxidizing prokaryotes (SOPs) and favor the growth of sulfate-reducing prokaryotes (Skousen et al., 2004; Xu & Mills, 2018; Zhang et al., 2022). This microbial shift may reduce dissolved metals in the water column as SRB promotes the precipitation of metals into sediment-associated forms such as metal sulfides. Conversely, under full-light conditions, photoautotrophic microbes increase oxygen availability, which supports enhanced SOP activity and promotes the oxidation of hydrogen sulfide (Ljungdahl et al., 2003; Skousen et al., 2004; Reddy & Delaune, 2008). This process may reduce the availability of H_2S needed to form insoluble metal sulfides, potentially limiting metal sequestration in sediments.

Despite extensive research on metal biogeochemistry in water bodies, there is a gap in understanding how microbial metabolic functions and natural community structure and environmental factors affect the sequestration of metals in wetlands (Xu & Mills, 2018; Rosemond et al., 2015; Richard et al., 2021). Microbial interactions can strongly influence sediment chemistry. Specifically, methanogens and sulfate-reducing prokaryotes (SRPs) can shape conditions that affect metal retention, often through competition with each other for substrates and the regulation of sulfide production (Lovley, 1983; Hines et al., 1989; Holmer & Nielsen, 1997). Furthermore, limited research has explored how these communities respond to varying light levels in metal contaminated wetlands. Kang et al. (2019) illustrated how variation in oxic versus anoxic conditions influences metal mobility in river systems, finding that anoxic conditions led to the release of metals such as lead, zinc, and iron , from sediments due to reduced redox potential and the dissolution of metal-oxide complexes, while oxic conditions promoted their adsorption from the water column back into sediments. While we know that environmental factors influence microbial communities in wetlands, the relationship between light availability and microbial mediation of metal interactions in wetlands remains poorly understood.

With mounting evidence of current and projected shifts in climate—potentially altering light availability and other key environmental conditions, the need to understand the complex interplay among microbial communities, environmental drivers, and metal cycling in wetlands is more critical than ever. This understanding is indispensable for ensuring the sustainable management of natural wetland ecosystems (Richard et al, 2021) and for determining best management practices for constructed ecosystem designs. Therefore, my research goal was to address the following question: How do environmental light availability conditions affect the capability of microbial communities to alter the fate of metals in wetlands? I hypothesized that if light influences microbial community composition, then light-exposed communities would experience increased potential for photosynthesis due to greater abundances of phototrophic organisms. The resulting increase in oxygen is expected to stimulate sulfur-oxidizing prokaryote (SOP) activity while suppressing sulfate-reducing prokaryotes (SRPs), leading to less hydrogen sulfide production and, consequently, decreased formation of copper sulfide particulates.

Wetlands differ not only in their exposure to environmental stressors but also in the history of contamination experienced by their microbial communities. Constructed wetlands, given their purpose can accumulate metals over time, potentially selecting for microbial taxa that are more tolerant to metal stress. In contrast, natural wetlands without a history of contamination may lack these metal-tolerant groups. Previous studies have demonstrated that sulfate-reducing bacteria and other metal-tolerant microorganisms can adapt to elevated metal concentrations, particularly in environments with high sulfate and heavy metal inputs, such as acid mine drainage systems (Martins et al., 2009). I hypothesized that a constructed wetland would exhibit higher richness and evenness of metal-tolerant microbial taxa compared to an uncontaminated natural wetland, and that this community composition would confer greater potential for functional resilience to additional copper exposure, maintaining or enhancing the wetland's capacity for metal removal.

To address these hypotheses, I examined two light regimes—natural diel cycles and complete darkness—and assessed their effects in microcosms established with water and sediment from both a metal-contaminated constructed wetland and an uncontaminated natural wetland. Focusing on copper metal contamination, I analyzed the consequential alterations in copper partitioning into water and sediment compartments and the associated changes in microbial community composition.

I analyzed microbial communities to help clarify their roles and predict their associations with different functional groups, including sulfur-cycling organisms, in mediating copper bioavailability under varying light regimes. By identifying conditions that enhance or inhibit copper sequestration, this research will support the development of more effective microbial-focused wetland designs and management strategies for mitigating metal contamination in freshwater ecosystems.

CHAPTER 2

METHODS

Field Sites and Sample Collection

The study took place at two wetlands, H-02 Wetland and Sarracenia Bay, located on the Department of Energy's Savannah River Site (Aiken, SC, USA; Fig. 1a). The H-02 constructed wetland was established in 2007 to sequester heavy metals, including Cu and Zn, from cooling water discharged by the National Nuclear Security Administration's Tritium Processing Facility. The constructed wetland consists of two main cells lined with gypsum (calcium sulfate) and planted with California bulrush (*Schoenoplectus californicus*) through which contaminated water collected in the upper retention basin flows. As the water moves toward the outflow over a period of 48 hours (Bach, Serrato, & Nelson, 2008), contaminants are removed through burial in the sediments (Fig. 1b). Sarracenia Bay is a natural depressional wetland (Carolina Bay) that rarely dries completely over the summer season (personal communication, S. Lance) and is located 15.05 km east of the H-02 wetlands (Fig. 1c). Neither wetland has tree canopy cover. The use of both a constructed and a natural wetland adds significant value by allowing comparison between systems with different histories, vegetation, and baseline contamination levels.

Water and sediment samples were collected on July 27, 2024, from both sites: H-02 and Sarracenia Bay. At site H-02, eight collection points numbered one through eight were selected, corresponding to the center of each of the four sections within two cells (Fig. 1b). Samples were taken from the upper three cm layer of water ~3 m wide margins between the wetland bank and the start of the bulrush plants. At Sarracenia Bay, sample collection started 1 m from the water edge, with eight collection points spaced 20.5 m apart along two parallel transects (transects were 10 m apart) through the widest part of the water body such that the transect ended in the center of the wetland (Fig. 1c).

At each sampling location, four water and four sediment samples were collected. Water samples were obtained by rinsing a 250 mL wide-mouth acid-washed (10% nitric acid bath) plastic bottle with wetland water at each collection site. The bottle was submerged below the water surface near the sediment bottom, the cap was removed to release any trapped gas, and the rinse water was poured away from the collection site. This rinsing process was repeated twice, then the water sample was collected using the same method. The collected water was poured through a 300 µm mesh filter into an acid-washed carboy. Wetland water parameters: depth, pH, conductivity, water temperature, and dissolved oxygen, were measured out in the field using a hand-held YSI ProDSS Multiparameter Digital Water Quality Meter (YSI Inc./ Xylem Inc., Ohio), and water depth at each collection point was recorded with a meter stick. This procedure was repeated for each collection point at both wetlands.

At each collection point, after water samples were collected, the upper sediment layer to a depth of 1 cm was collected into an ethanol-sterilized bucket. Both water and sediment samples were transported to the lab on ice in coolers. At the lab, water and sediment samples from each site were homogenized separately. Sediment was sieved through an acid-washed plastic soil sieve with a 6.5 mm mesh size. Homogenized water and sediment samples from the field baseline (hereafter referred to as “Field” samples) of each wetland were stored and processed at the laboratory for DNA, nutrient analysis, metals, and chlorophyll-*a*.

Microcosm Set-up

On July 30, 2024, a total of 34 microcosms were established. Half of the microcosms were created using H-02 Wetland water and sediment and the other half were created using Sarracenia Bay water and sediment. The microcosms were created using autoclaved 473 ml wide-mouth glass bottles. Oxygen sensor spots SP-PSt7-NAU (PreSens, Inc. Germany) were adhered to the side of each experimental microcosm (2 cm above the sediment surface) and microcosms were filled with 60 mL of sieved, homogenized sediment from its respective wetland (~25.8 g for H-02 and ~4.9 g Sarracenia sediment dry weight). Wetland water (425 mL) was added to each microcosm while minimizing sediment disturbance. Six bottles (three from each wetland site) were designated as background bottles to monitor contamination and bottle effects outlined in Sub-section: Environmental manipulation and copper addition.

The microcosms were initially stored in the dark at 4 °C for two days to acclimate and facilitate the settling of sediment particles. A subset of four bottles (two per wetland source) were then destructively sampled to assess bottle effects on key measurements using the same parameters and methods as for field sample processing. The remaining 24 microcosms were randomly assigned to the following treatment groups: H-02 Light, H-02 Dark, Sarracenia Bay Light, and Sarracenia Bay Dark. Six bottles were assigned to each group experimental group and four additional microcosms were established with the ltrapure water (MilliQ, SYNSVR000, Millipore Synergy Water Purification System, Remote Pure UV Ultrapure, Millipore Corporation, Burlington, MA USA) and no sediment negative controls (two for the light treatment and two for the dark treatment).   In addition to the 20 experimental microcosms, we included four background controls with Milli-Q water (two with metal added), three lab controls with wetland sediment and water but no added metal (from both wetlands), and field samples for comparison.

To prevent external metal contamination, all materials used for constructing and sampling microcosms were either certified metal-free or acid-washed (10% nitric acid).

Environmental Manipulation and Parameters

After set-up and acclimation, microcosms were incubated in the H-02 wetland for the eight-day duration of the experiment. Microcosms were divided into regular diel cycle light exposure (referred to as "light") and no light exposure ("dark") groups. We conducted the experiment in the wetland environment to better reflect natural conditions. This approach allowed us to capture factors like natural light availability, which would be difficult to replicate accurately in a laboratory setting. Bottles were incubated only in H-02, rather than both wetlands, primarily due to restrictions on water quality. Specifically, concerns were raised about introducing bottles containing copper and other H-02 contaminants into a natural wetland environment, which is a critical amphibian habitat. Twelve microcosms were designated for light exposure (six from H-02, six from Sarracenia Bay, and two ultrapure water controls), and twelve were assigned to dark exposure (six from H-02, six from Sarracenia Bay, and two ultrapure water controls). The dark microcosms were wrapped in light brown duct tape to match the sediment color and block out light while minimizing heat absorbance. Microcosms were deployed at the H-02 wetlands in cell 1, section 1 (Fig. 1b). Each bottle was secured to a bamboo pole and placed in randomized batches resting on the sediment surface (Appendix 1).

To understand wetland environmental parameters, data were collected by a HOBO MX2202 temperature and light logger (Onset Computer Corporation, Firmware Version 59.140) deployed at the inflow side of the H-02 wetland in Cell 1, Block 1 (Fig. 1b). The sensor recorded temperature (°C) and light intensity (lux) using HOBO Connect software (Version 2.0.0) every 10 minutes from August 01, 2024, to August 10, 2024. From this dataset, the average daily light intensity (lux) and the duration of light exposure in hours were determined. Throughout the experiment, dissolved oxygen measurements were taken daily at dawn, noon and dusk (0600, 1200, and 1900). The pH (Fisherbrand accumet AE150 Benchtop pH Meter) was also measured at the setup and breakdown stages for each microcosm.

Experiment Timeline and Copper Addition

Microcosms were destructively sampled at four timepoints: immediately after microcosm set-up (July 30, 2024) (background microcosms only), at day zero which occurred after the two-day microcosm acclimation and sediment settling (background microcosms only), after four days of experimental treatments, and after eight days of experimental treatments. For each destructive sampling, microcosms were collected from the field, transported to the laboratory in a cooler, and samples were taken as detailed below. The remaining 15 microcosms had copper spikes added to induce metal contamination effects. This was done to separate the effects of light treatment from metal addition.

Specifically, at noon, 5.0 mL of 10.7 µg Cu/ml dissolved copper (as copper sulfate, $CuSO_4$) was added to each remaining microcosm to reach the upper limit of metal concentrations previously recorded in H-02 (31.7 µg Cu/L) as determined by Xu and Mills (2018). Copper solution was made using the corresponding field wetland water filtered through 0.2 µm pore filters (Supor 200, PALL Corporation) or ultrapure water for negative controls. On the eighth day, these remaining microcosms were deconstructed for samples.

Microcosms to be destructively sampled were removed at noon on collection days. Sample collection from microcosms included microbial community sampling (water for DNA analysis), water for chlorophyll-*a*, water for nutrient analyses (dissolved organic carbon (DOC), nitrate/nitrite, and ortho-phosphate), and water and sediment for copper concentrations. These sample collections were completed for each sacrificed microcosm and processed as described in Sub-section: Environmental manipulation and copper addition.

Sample Processing and Analysis

For inorganic nutrient analysis, unfiltered water samples (100 mL) were preserved with sulfuric acid (pH ≤ 2) at the time of collection. Acidified water samples from both field collections and all microcosms were collected and stored in a laboratory refrigerator (4°C) for no more than two days until transport to the Phinizy Center for Water Sciences (Augusta, GA, USA). Samples were analyzed at the Center for Total NOx (nitrate/nitrite) using EPA method 353.2 and ortho-phosphate concentrations using EPA method 365.1.

For dissolved organic carbon analysis, a 45 mL water sample from field wetlands and each microcosm was collected and stored at -20 °C until analysis. Water samples were filtered through 0.2 µm pore filters (Supor 200, PALL Corporation) and immediately analyzed on a Shimadzu Total Organic Carbon analyzer (SHIMADZU CO, Columbia, MD) at Savannah River Ecology Laboratory.

Water from the field and microcosms (50 ml) was filtered using a vacuum pump and GF/F filters (0.7µm pore size, 47mm) (WP6211560, EMD Millipore Corporation, Burlington, MA, USA). Filters were stored in 15 mL Falcon tubes wrapped in aluminum foil to protect chlorophyll-*a* from light and frozen at -20°C for at least three hours. Following Kohler et al.

2022 extraction methods, filters were thawed, submerged in 7.5 mL of 90% ethanol, and sonicated for 30 seconds to enhance extraction efficiency, followed by a 10-minute incubation in a 70°C water bath. The tubes were then cooled at 4 °C for at least one hour. A 200 µL aliquot was then transferred to a 96-well clear plate and measured at 435 nm excitation and 676 nm emission (bandwidth ≤3 nm). Absorbance was recorded at 665 nm (chlorophyll-*a*), 649 nm (chlorophyll-a), and 750 nm (turbidity). Samples were checked to confirm that the absorbance at 750 nm did not exceed 0.005. The Welschmeyer non-acidification method was used to prevent underestimation, and chlorophyll-*a* concentrations were calculated, following Wintermans & De Mots (1965).

For copper analysis of media, a 45 mL sample of each unfiltered water and sediment was collected in metal-free 50 mL centrifuge tubes from field samples and microcosms and stored at -20°C until analysis.

For water samples, samples were thawed in a refrigerator and acidified with trace metal grade nitric acid to a final concentration of 2% (v/v). Acidified samples were held for at least 16 hours to ensure complete dissolution of metals. For dissolved copper analysis, samples were filtered using 0.45 µm metal-free filters (Millipore Sterivex-HV) prior to acidification. Copper concentrations were quantified using inductively coupled plasma mass spectrometry (ICP-MS) following EPA Method 200.8.

Sediment samples were digested using microwave-assisted acid digestion following EPA Method 3051A. Approximately 0.250 g of dried, homogenized sample was weighed into acid-cleaned MARSXpress vessels, and 10 mL of trace metal-grade nitric acid was added. Samples were allowed to pre-digest for 15–30 minutes before being sealed and digested using a CEM

MARS 6 microwave digestion system. After cooling, digestates were transferred to 50 mL metal-free centrifuge tubes and diluted to volume with ultrapure water (Milli-Q). A second dilution was performed as needed for ICP-MS analysis. Quality control measures included method blanks, certified reference materials (a tomato leaf standard NIST 1573a for Sarracenia Bay and the PACS-3 standard for H-02), and matrix spikes.

Copper concentrations in the water and sediment subset samples were measured in copper in part per million (ppb). Duplicate water and sediment samples were included after every 20th sample. All ICP-MS analyses were conducted at the Savannah River Ecology Laboratory Analytical Services.

The mean detection limit (MDL) for all water samples was 0.210 µg/L for Cu. Copper concentrations in laboratory blanks were consistently below detection. The mean relative percent difference (RPD) between replicate water samples was 2% for Cu. However, some replicate sets exhibited higher variability (e.g., 176% RPD for Cu in one sample). The higher RPD observed between copper replicates may be due to differences in how much the samples were shaken, potentially causing uneven suspension of copper particulates. Across all replicates, the average RPD for copper was approximately 45%.

The method detection limit across H-02 sediment samples (N = 15) was 0.137 mg Cu kg^{-1}. All blank values were below this detection threshold. The mean relative percent difference (RPD) between duplicate samples was 13% for Cu (SD = 11.3%, n = 2), with one pair scoring 5% RPD and another pair showing 21%. Spike recoveries for Cu averaged 106% (SD = 2.83%, n = 2), based on 10 ppb spike additions. Certified reference material (PACS-3) recoveries for Cu averaged 103% (SD = 5.7%, n = 2).

The method detection limit across Sarracenia Bay sediment samples (N = 16) was 0.0329 mg Cu kg^{-1}, and blank values were consistently below this threshold. The mean relative percent difference (RPD) between duplicate samples was 1.48% for Cu (SD = 2.12%, n = 1). Additional replicate sets showed higher RPDs (e.g., 29% for Cu). Spike recoveries for Cu averaged 100.3% (SD = 0.25%, n = 2), based on 20 ppb spike additions.

DNA Sample Processing and Sequencing

From field and microcosm samples, DNA was collected on filters from 200 mL of water by filtering through 0.2 µm pore filters (Supor 200, PALL Corporation), using a vacuum pump (EMD Millipore Corporation, Burlington, MA, USA). Filters (water microbial community) were stored at -20°C until further processing. Water filters were extracted using a DNeasy PowerWater kit (Qiagen, Germantown, MD) according to the manufacturer's recommendations. Negative extraction controls containing no sample were processed for each sample set (20 samples per set) and sequenced to check for contamination.

After extraction, DNA was eluted with 50 µL of elution buffer and quantified using the Quant-IT PicoGreen dsDNA Assay Kit and a Synergy HTX Multi-Mode Microplate Reader (BioTek). Extracted DNA was shipped to the University of Delaware Ammon-Pinizzotto Biopharmaceutical Innovation Center, DNA Sequencing & Genotyping Center (Newark, DE 19713) for sequencing using the NextSeq 2000 Illumina Platform with 600-cycle P1 (PE 300bp) using primers 515F (Parada et al. 2016) and 806R (Apprill et al. 2015). These primers were used as they target the V4 region of the 16S rRNA gene, which is commonly used for characterizing bacterial and archaeal community composition. For the extraction blanks and controls, these were added at 0.1 x the sample library.

We generated demultiplexed sequence data for each of our samples. The sequencing plate had independent dereplication, filtering, and trimming to 250 bp using Cutadapt (version 17.1) (Martin, 2011), followed by error learning and sample inference in the R package dada2 (version 1.16) (Callahan et al., 2016). This pipeline produced merged, denoised, chimera-free amplicon sequence variants (ASVs) from paired-end FASTQ files. We assigned taxonomy using the SILVA database (version 138.1, 99% identity threshold) (Quast et al., 2013; McLaren and Callahan, 2021). We processed negative controls with the decontam R package (Davis et al., 2018) and removed 114 likely contaminants with a score >0.52. Additionally, we removed ASVs assigned to chloroplasts, mitochondria, and Eukarya.

After removing sequencing artifacts (e.g., long CCC repeats), singletons defined as sequences that only occurred once in all samples, and subsetting data, there were 40,088 taxa remaining. Sequencing coverage was assessed using rarefaction curves, which indicated sufficient depth across all samples (Appendix 2). For alpha diversity, samples were rarefied to 187,521 abundance per sample using phyloseq_mult_raref (microbiome package, Lahti & Shetty, 2012–2019).

To infer potential metabolic functions of microbial communities, we used the Functional Annotation of Prokaryotic Taxa (FAPROTAX) database (Louca et al., 2016). FAPROTAX maps taxonomic information to ecologically relevant functional groups based on published literature, allowing us to estimate the abundance of metabolic pathways such as sulfur oxidation, sulfate respiration, photoautotrophy, and methanogenesis. We applied the FAPROTAX pipeline to our taxonomic table (derived from 16S rRNA gene sequencing) to generate a table of predicted functional group abundances. The resulting functional profiles were analyzed for differences across treatments (e.g., light vs. dark) using non-parametric statistical tests as sequencing data are compositional and do not meet assumptions of normality. To minimize the influence of extremely rare taxa and reduce statistical noise, sequencing data were filtered to include only AVSs assigned to these functional groups. The AVS table was normalized to relative abundance within each sample using transform sample counts, and taxa missing in all replicates of a group were excluded.

Statistical Analysis

All statistical analyses were performed using R version 4.3.1 (R Core Team, 2023) with the aid of the University of Georgia's Georgia Advanced Computing Resource Center's Sapelo2 Linux cluster.

To assess the validity of the statistical models, several assumptions were checked. These included the normality of residuals, linearity between predictors and outcomes, homoscedasticity of residuals, and goodness of fit. To test these assumptions, normality was assessed using the Shapiro-Wilk test when applicable (shapiro.test) (R Core Team, 2023), and Q-Q plots and residual plots were used to check the residuals for normality and homoscedasticity. The coefficient of determination (R^2) was computed using the r. Squared GLMM function for model evaluation (R Core Team, 2023). Statistical significance was defined as a p-value of < 0.05.

To determine whether the light and dark treatments influenced environmental changes in the microcosms, we assessed the environmental parameters. One linear mixed-effects model(lme4 package, Bates et al., 2015) was constructed to determine treatment effects and additional environmental parameter relationships to the dissolved oxygen trends. The model used light treatment, wetland source, copper addition , hours of light exposure before sampling (extrapolated from sensor data), as fixed variables, while average daily light intensity (extrapolated from sensor data) and time of measurement were included as random variables. This was done to differentiate between normal environmental effects and the true effects of the treatment groups. To address discrepancies in data normalization assumptions, dissolved oxygen measurements were log-transformed.

Chlorophyll-*a* concentrations were analyzed as a proxy for autotrophic growth and metabolic activity under light and dark conditions. Chlorophyll- *a* concentration was the dependent variable, with light treatment, wetland source and copper addition as fixed effects . Additionally, the interaction between copper addition and light treatment was analyzed. To address normality issues in the original model and to meet the assumptions, chlorophyll-*a* values were log-transformed to improve residual normality. Light exposure effects on chlorophyll-*a* were determined by a model using sensor log data. This was done to differentiate between normal environmental effects and the true effects of the treatment groups.

To determine how light exposure influenced the dynamics of copper flux between the sediment and water compartments, the sediment-to-water concentration ratios for copper were assessed. These values were estimated based on the sediment dry mass and water volume in each microcosm. Ratios were calculated by dividing the total copper in water by the total copper in sediment in each microcosm. The model was a linear mixed-effects model (lme4 R package, R Core Team, 2023) that accounted for both fixed effects: light treatment and copper addition (and their interactions) and Wetland Source (H-02 Wetland or Sarracenia Bay).

To examine the effects of light treatment, wetland source, and their interaction on microbial community alpha diversity, I ran two linear models in R with community richness or evenness as the response variables (v4.3.2; R Core Team, 2023). The predictor variables included light treatment (light or dark), wetland source (e.g., H-02 or Sarracenia Bay), and their interaction. Richness was calculated as observed ASV counts, and evenness was computed using Pielou's index from Shannon diversity metrics. Both measures were extracted using the phyloseq R package (v1.46.0; McMurdie & Holmes, 2013).

To understand treatment effects on beta diversity, the extent to which copper addition explained the variability in the microbial community for each wetland source relative to other environmental parameters was analyzed. For this analysis, ASVs occurring less than 10 times in the dataset were removed and the dataset was then cumulative sum scaling normalized with the metagenomeSeq R package version 1.38.0 (Paulson et al., 2013). Then, PERMANOVA was conducted on a Bray–Curtis dissimilarity distance matrix using light, wetland source, copper addition, and time as explanatory variables with 999 iterations (Anderson, 2017), implemented via the adonis2 function in the vegan R package (Oksanen et al., 2025; version 2.7-0). To evaluate how different light treatments influence variation in microbial community structure, ordination was performed using both non-metric multidimensional scaling (NMDS) and principal coordinates analysis (PCoA) based on the Bray-Curtis dissimilarity matrix, implemented via the phyloseq package (v1.46.0; McMurdie & Holmes, 2013) and vegan package (v2.6-4; Oksanen et al., 2022) in R (v4.3.1; R Core Team, 2023). Environmental vectors including copper, dissolved organic carbon, chlorophyll-*a*, pH, nitrate, and ortho-phosphate were fitted to the ordination space using the envfit function with 999 permutations to assess correlations.

To determine treatment effects on predicted functional groups, functional group abundances derived from FAPROTAX annotations were first filtered to retain groups with sufficient representation across samples. These abundances were then merged with taxonomic data at the Order level (or in the case of Sulfur Oxidizing microorganisms, on a species level) to focus on relevant taxa. The data were normalized to relative abundances and log-transformed to meet analysis assumptions. For each functional group, a Wilcoxon rank-sum test was performed to assess differences in abundance between light treatments before or after copper addition. Subsequently, Orders associated with functionally significant groups were also tested using Wilcoxon rank-sum tests. The same approach was applied to compare differences in abundance between wetland sources within light and dark treatment groups. P-values were adjusted for multiple comparisons using the Benjamini-Hochberg method.

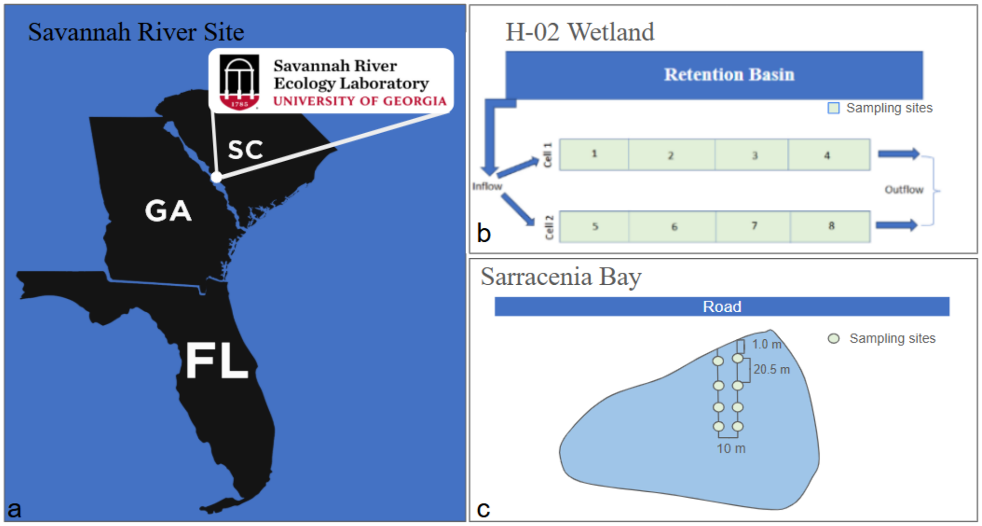

Figure 1. Study sites in two wetlands where field water and sediment samples were collected at the Savannah River Site, Aiken, South Carolina, USA. (a) Savannah River Site location, (b) H-02 Constructed Wetland site map (not to scale), and (c) Sarracenia Bay sampling site map (not to scale) with parallel lines of sample points located one meter from the water edge and 20.5 m apart with 10 m between parallel lines.

CHAPTER 3

RESULTS

Light exposure modified the ratio of copper in sediment-to-water, and this pattern differed by whether copper had been spiked into the microcosm. Table 1 shows mean and Standard error scores. For both wetlands, prior to copper addition, light-exposed microcosms had copper in sediment-to-copper in water ratios higher by 1.29 (S.E. = 0.227, t = 5.709, p = 0.011, R^2m = 0.98, R^2c = 0.933) compared to those in the dark treatment (Fig. 2). In contrast, the combination of copper addition and light treatment resulted in an average decrease in the ratio by -2.619 (S.E. = 0.3205, t = -8.173, p = 0.004, R^2m = 0.97, R^2 a= 0.93) compared to the dark treatment after copper addition. The interaction of light treatment and copper addition also significantly influenced these ratios resulting in an estimated negative effect of 2.62 (S.E. = 0.321, t = -8.173, p = 0.004, R^2m = 0.97, R^2 a= 0.93) in the light exposure and copper addition group (Appendix 4).To contextualize, background sediment to water copper ratio prior to copper addition was 1.24 (S.E = 0.72) in H-02 and 2.29 (S.E =1.11) in Sarracenia Bay. These values reflect baseline variability in copper levels across wetlands.

The varying treatments altered some environmental parameters in the microcosms for both wetland sources including chlorophyll-*a,* ortho-phosphate and dissolved oxygen (Appendix 3 and Appendix 5). The median percent oxygen was higher in the dark treatment (77.0% ± 28.7 SE) compared to the light treatment (45.9% ± 24.8 SE), suggesting that light exposure may reduce oxygen saturation in these wetland systems. Light treatment and copper addition significantly influenced log-transformed chlorophyll-*a* concentrations in the microcosms (Fig.

3). On average, light-exposed microcosms contained 0.696 μg/L more chlorophyll-*a* (log) (S.E. = 0.21, t = 3.34, df = 41.42, p = 0.002, $R^2m = 0.38$, $R^2c = 0.38$) compared to the dark treatment group before the copper addition. In contrast, the combination of copper addition and light treatment resulted in an average decrease of 0.717 μg/L in chlorophyll-*a* (log) (S.E. = 0.29, t = -2.49, df = 41.42, p =0.002, $R^2m = 0.38$, $R^2c = 0.38$) compared to dark treatments with copper added.

The linear model of log-transformed ortho-phosphate concentrations explained a significant portion of the variation in ortho-phosphate concentrations ($F(4, 41) = 17.44$, $p < 0.001$, R^2 adjusted = 0.59). Copper addition also resulted in a significant reduction in ortho-phosphate (Estimate = –1.15, p = 0.003). In contrast, the main effect of light treatment was not significant (Estimate = 0.13, p = 0.73).

Light treatment significantly reduced $\log(O_2)$ levels (Estimate = –0.25, p = 0.0119). A marginally non-significant negative trend was observed for high light availability (hlight; Estimate = –0.46, p = 0.0606). The model accounted for random variation across sampling conditions by including random intercepts for average light availability (variance = 0.537) and time (variance = 0.428), with a residual variance of 0.781. Overall, the model explained a moderate portion of the variance in the data (marginal $R^2 = 0.036$, conditional $R^2 = 0.569$), and demonstrated a good fit (REML criterion = 896.1), with scaled residuals ranging from –2.60 to 3.39.

Microcosms made using Sarracenia Bay water and sediment exhibited trends for several environmental variables that differed from those in microcosms with H-02 Wetland media. Sarracenia Bay microcosms had a trend of higher chlorophyll-*a* concentrations compared to H-

02 microcosms, with an average increase of 0.468 μg/L (S.E. = 0.14, t = 3.25, df = 41.4, p = 0.017, R^2m = 0.38, R^2c = 0.38). Relative to H-02 Wetland microcosms, Sarracenia Bay microcosms exhibited higher copper in sediment-to-copper in water ratios, with an average increase of 0.94 (S.E. = 0.1602, t = 5.869, p = 0.010, R^2m = 0.97, R^2 a= 0.93). The wetland microcosms also exhibited higher log chlorophyll-*a* concentrations compared to H-02 microcosms, with an average increase of 0.468 μg/L (S.E. = 0.14, t = 3.25, df = 41.4, p = 0.017, R^2m = 0.38, R^2c = 0.38). Similarly, Sarracenia Bay trended to have higher dissolved oxygen levels, with an estimated 1.184% higher log oxygen compared to H-02 Wetland (S.E. = 0.58, df = 15, t = -2.037, p = 0.060, R^2 m= 0.35, R^2 adjusted = 0.57). Wetland source also had a significant effect on ortho-phosphate with samples from Sarracenia Bay having significantly lower ortho-phosphate concentrations than those from H-02 (Estimate = –1.99, $p < 0.001$).

Alpha Diversity

Bacterial community alpha diversity metrics of richness and evenness were significantly influenced by light treatment (Fig. 4). Dark microcosms had an estimated median richness of 4,597 ASVs (S.E. = 381), whereas those exposed to light had an estimated median of 9,169 ASVs (S.E. = 1745) (Total model p = 0.01, R^2m = 0.50, R^2c = 0.39, F = 4.505, df =18). The light treatment significantly increased microcosm bacterial community richness by an average of 4,805 ASVs (S.E. = 1593, linear mixed model: t = 3.016, p = 0.007). Whereas wetland sources did not significantly change in community richness (p = 0.61).

Community evenness also varied by light treatment (Total model p = 0.12, R^2m = 0.26, R^2c = 0.14, F = 2.216, df =18). Light exposed microcosms had lower estimated Pielou's evenness (0.957, S.E = 0.007) than those kept in the dark (Pielou's evenness 0.962, S.E = 0.003, Wilcoxon rank sum pairwise comparison, p = 0.04). Whereas community evenness did not differ between the two wetland sources (p = 0.73).

Beta Diversity

Non-metric multidimensional scaling (NMDS) was used to visualize differences in microbial community composition across treatments. The NMDS ordination achieved a fit with a stress value of 0.00009.Such extremely low stress values are often an artifact of small sample sizes and may not reliably indicate the ordination's robustness.. Although samples showed some spatial separation, no distinct clustering was observed by copper addition, light treatment, or wetland source.

Due to the small sample size, NMDS ordination results should be interpreted cautiously, to further support these findings a Principal Coordinates Analysis (PCoA) was used to explore variation in microbial community composition based on Bray–Curtis dissimilarities. The first two axes explained 42.2% and 7.2% of the total variation, providing a reasonable two-dimensional representation of differences among samples (Fig. 5). While some separation among samples was visually apparent, no distinct clustering patterns emerged by copper addition, light treatment, or wetland source—consistent with the PERMANOVA results. The broad distribution of samples across the ordination space suggests high within-group variability and weak structuring by the tested treatment factors. Environmental vectors fitted to the PCoA ordination revealed no significant correlations between specific environmental variables and microbial community patterns (Table 1).

Metal exposure, light treatment, and wetland source did not have a combined or individual statistically significant effect on community composition (Table 3). Copper addition did not show a significant effect ($R^2 = 0.069$, $p = 0.178$), suggesting a limited influence on community variation. Light treatment and wetland source were not significant explanatory factors for microbial community composition (Table 3).

Functional Groups

There were 40 identified functional groups from the dataset. Overlapping of similar or identical predicted functional genes across groups was common, due to contributions to multiple predicted functions. Differences in relative abundances between light and dark treatment groups occurred in 14 functional categories (Table 4, non-significant values in Appendix 6). The functional categories, 'Respiration of sulfur compounds', 'Sulfur respiration', 'Oxygenic photoautotrophy', 'Photosynthetic cyanobacteria', 'Phototrophy', 'Methanogenesis', , 'Hydrogenotrophic methanogenesis', 'Acetoclastic methanogenesis', 'Dark hydrogen oxidation', 'Methanogenesis by CO_2 reduction with H_2', and 'Methanogenesis by disproportionation of methyl groups' all comprised a greater relative proportion of the known functions after copper addition in the light treatment compared to the dark treatment with P values all below 0.01 (Table 4, non-significant values in Appendix 7). Additionally, 'Chemoheterotrophy' had greater relative abundance in the light treatment before copper addition and greater relative abundance in the dark treatment after copper addition. There were no significant differences between wetland sources (H-02 and Sarracenia Bay) in 14 functional categories grouped by light treatment (Wilcoxon rank-sum tests, Appendix 6).

Sulfur respiration functions were significantly enriched in light-exposed microcosms compared to dark treatments under copper-amended conditions (Table 4). Although the overall difference was modest, median log abundance values were slightly higher in light treatments (median = 1.11) than in dark treatments (median = 1.00), indicating a statistically significant light-associated increase in sulfur respiration potential. Further taxonomic analysis of the 'Sulfur respiration' functional group—which also overlapped entirely with 'Respiration of sulfur compounds' indicated that, out of the 12 identified bacterial orders, four exhibited significant differences between light and dark treatments following copper addition (Table 5, non-significant values in Appendix 8). *Desulfovibrionales* and *Desulfomoniales* had greater relative abundance in the dark, while *Syntrophales* and *Desulfobaccales* were more relatively abundant in the light treatment conditions.

Photosynthesis-related functional groups had significantly enriched in light-exposed microcosms compared to dark controls under copper-amended conditions (Table 4). Median relative abundance values were higher in light treatments (median = 1.07) than in dark treatments (median = 0.84), indicating a statistically significant light-associated increase in photosynthesis potential. Further taxonomic analysis of the 'Oxygenic photoautotrophy' functional group — which also overlapped entirely with 'photoautotrophy', 'phototrophy', and 'photosynthetic Cyanobacteria'— indicated that, out of the four identified bacterial orders, three exhibited significant higher log relative abundances in the light treatment compared to dark (Table 4). *Micrococcales* and *Verrucomicrobiales* had greater relative abundance in the dark treatment following copper addition while *Sphingomonadales* had greater relative abundance in the dark treatment both before and after copper addition.

Functions related to methane production or consumption had significantly enriched in light-exposed microcosms compared to dark treatments under copper-amended conditions ($p < 0.05$). Further taxonomic analysis of the 'Methanogenesis' functional group, used as the representatives of these functional groups had median abundance values in light treatments of

1.43 and 1 in the dark treatments, indicating a statistically significant light-associated increase in photosynthesis potential. Of the ten identified bacterial orders, two exhibited significant differences in log abundances in the light compared to the dark treatment, *Methanobacteriales, and Methansarcinales* both had significantly higher relative log abundances in the dark exposed microsomes before and after metal addition (Table 5).

The Chemotrophic functional group relative abundances were significantly lower in light treatments compared to dark treatments before copper addition and higher after copper addition (Table 4). Of the 16 identified bacterial orders, 10 exhibited significant differences in log relative abundances in the light compared to the dark treatment. *Peptostreptococcales, Flavobacteriales, Anaerolineales, Holophagales, Methanosarcinales, Methylococcales, Oscillospirales, Sphingomonadales, Verrucomicrobiales* all had higher log relative abundances in the dark treatment groups after copper addition (Table 5).

Only one Order, *Burkholderiales*, had higher log relative abundance in the dark treatment compared to the light exposed groups before and after copper addition. While Sulfur Oxidizing was not a functional group category, several species within the *Burkholderiales* that can oxidize sulfur compounds were identified: *Sulufritalea*, *Sulfurisoma*, and *Thiobacter.* Despite *Burkholderiales* having higher relative abundances in the dark treatment, both *Sulufritalea*, and *Sulfurisoma* had higher overall percent relative abundances in light treatments: 6.9% and 29.0% compared to dark treatments: 0.07% and 26.3% respectively. Note however, p-values could not be assigned because the analysis is done at the genus level, where many genera have low or highly variable abundances across samples, resulting in insufficient statistical power to detect differences between treatments.

Table 1. Mean (± SE) copper concentrations by light treatment, wetland source, and copper addition.

Light Treatment	Substrate	Copper addition	Wetland	Mean Copper µg/L	SE
Dark	Water	No	Sarracenia Bay	4.080	0.557
Dark	Water	Yes	Sarracenia Bay	37.643	10.946
Light	Water	No	Sarracenia Bay	5.016	0.575
Light	Water	Yes	Sarracenia Bay	19.995	6.339
Dark	Water	No	H-02	46.243	16.054
Dark	Water	Yes	H-02	43.046	3.447
Light	Water	No	H-02	31.854	6.643
Light	Water	Yes	H-02	67.801	29.682
Light Treatment	**Substrate**	**Copper addition**	**Wetland**	**Mean Copper µg/kg**	**SE**
Dark	Sediment	No	Sarracenia Bay	18.666	1.006
Dark	Sediment	Yes	Sarracenia Bay	20.726	1.135
Light	Sediment	No	Sarracenia Bay	15.232	3.791
Light	Sediment	Yes	Sarracenia Bay	21.043	0.809
Dark	Sediment	No	H-02	43.563	9.546
Dark	Sediment	Yes	H-02	35.788	11.285
Light	Sediment	No	H-02	41.985	2.019
Light	Sediment	Yes	H-02	26.742	2.701

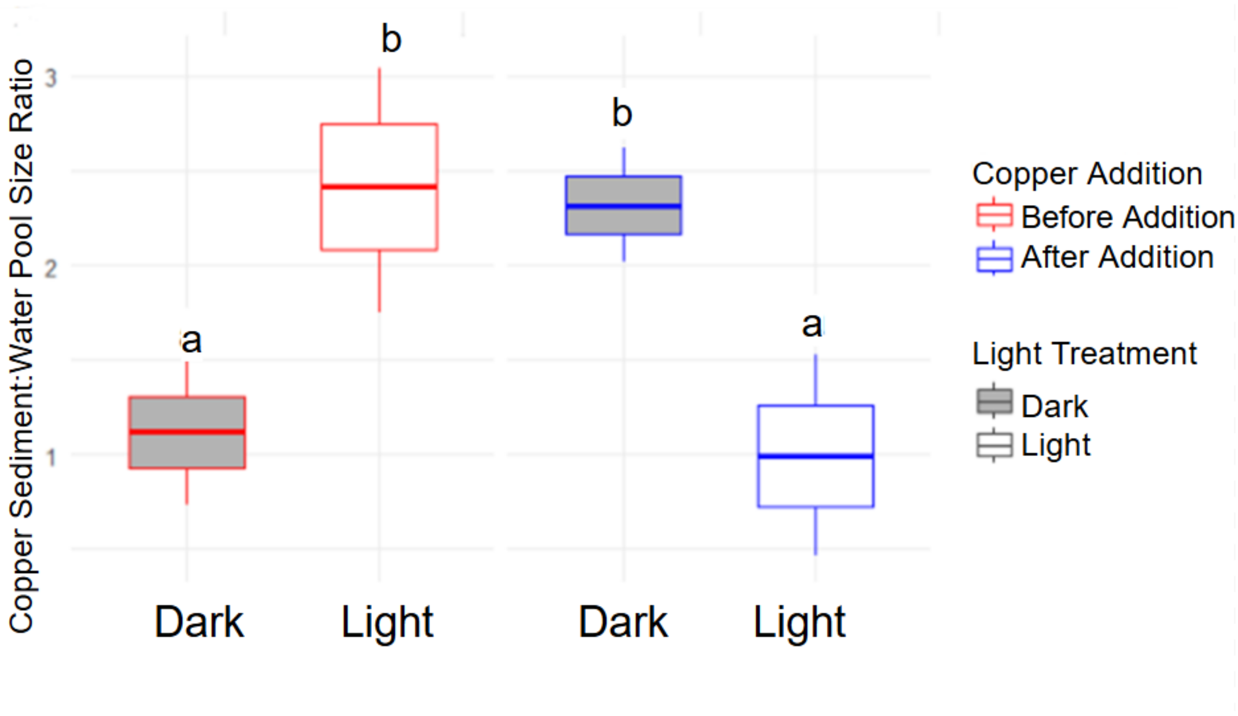

Figure 2. Boxplot of the copper sediment-to-water pool ratio in light and dark treatments before (red) or after (blue) copper addition (None = no copper added, Added = copper added). The predicted values and their associated confidence intervals were derived from the Metal vs Light treatment model (Appendix 5). Different letters denote statistically significant differences between groups ($p < 0.05$).

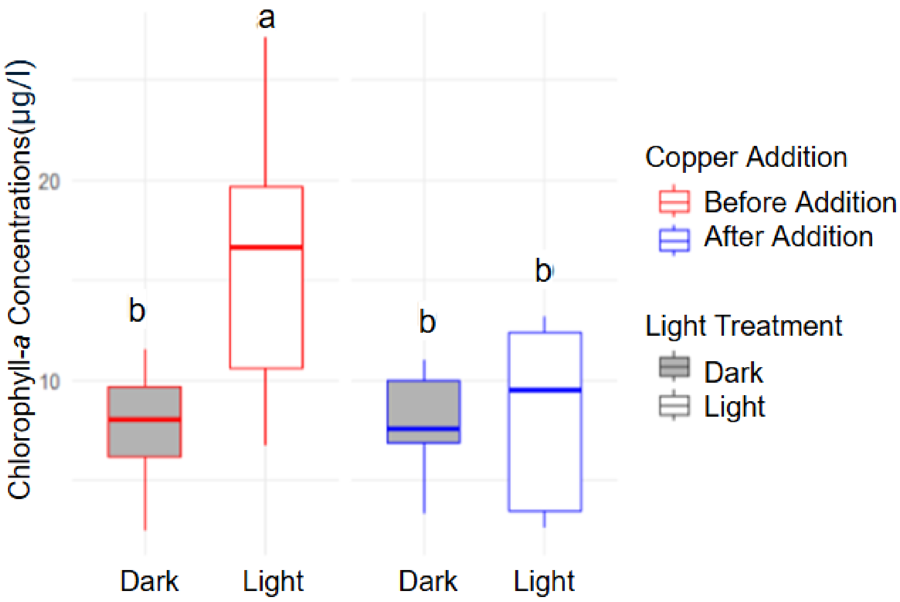

Figure 3. Boxplots of measured chlorophyll-a concentrations (µg/L) in microcosms exposed to different light treatments and copper additions. Data are grouped by light treatment (Dark = shaded, Light = unshaded) and metal addition (None = no copper added, added = copper added), with chlorophyll-a shown on the original (non-log) scale. Points represent individual measurements. Statistical differences among groups were assessed using a linear model on log-transformed chlorophyll-a, including main effects of light treatment, copper addition, and wetland source, as well as their interaction (see Appendix 3). Different letters indicate statistically significant differences between groups ($p < 0.05$).

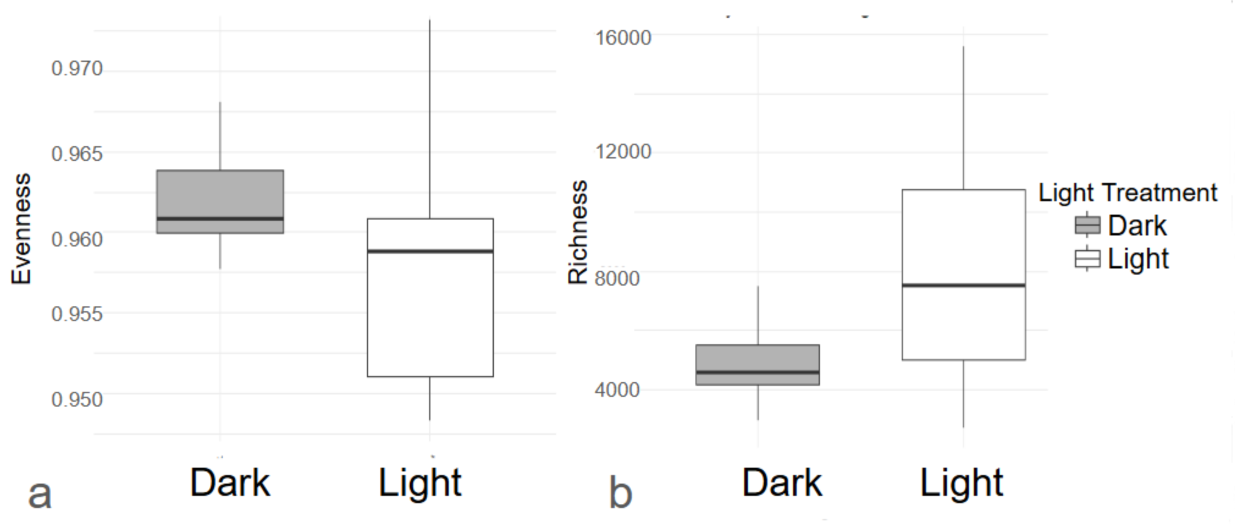

Figure 4. Boxplots of bacterial community alpha diversity in wetland microcosms with light and dark treatments for a) Pielou's Evenness and b) observed richness. Both alpha diversity metrics differ significantly between treatments ($p < 0.05$).

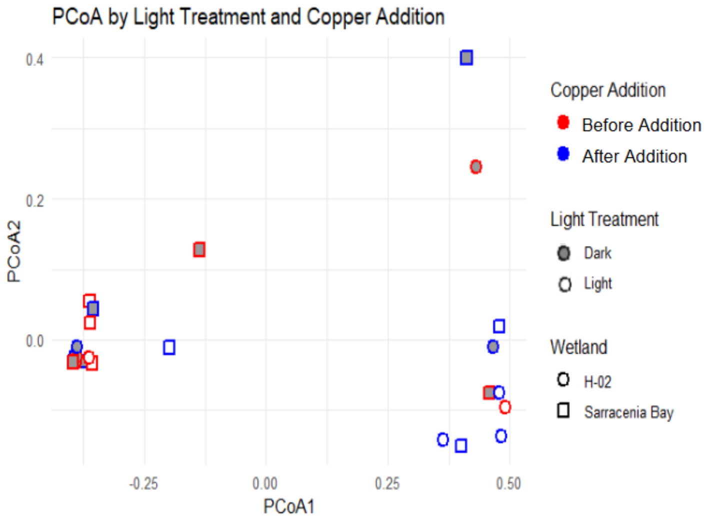

Figure 5. Principal coordinates analysis plot displaying bacterial community composition in microcosms in dark and light treatments and wetland source with or without added copper.

Table 2. Environmental variables correlated with PCoA ordination (Bray-Curtis distance).

Variable	Axis.1	Axis.2	R^2	p-value
Cu (ppb)	0.22954	-0.9733	0.1874	0.125
DOC (mg/L)	0.09845	0.99514	0.044	0.64
Chla (µg/L)	-0.98067	0.19568	0.0307	0.738
pH	-0.0547	0.0213	0.8394	0.629
Nitrate (mg/L)	0.40938	-0.91236	0.0667	0.501
Orthophosphate (mg/L)	0.7321	-0.6812	0.1255	0.298

*Copper (Cu), (DOC) Dissolved Organic Carbon (DOC), Chlorophyll-*a* (Chla)

Table 3. PERMANOVA summary of microbial community composition

Factor	Df	Sum of Squares	R²	F	p-value
Copper Addition	1	0.4323	0.069	1.55	0.178
Light Treatment	1	0.3360	0.053	1.19	0.236
Wetland Source	1	0.2473	0.039	0.86	0.390
Combined (Model)	3	0.9903	0.158	1.19	0.283

Table 4. Significant results of Wilcoxon signed-rank analysis comparing functional categories of median log-transformed relative abundances between light and dark treatments, with or without copper addition

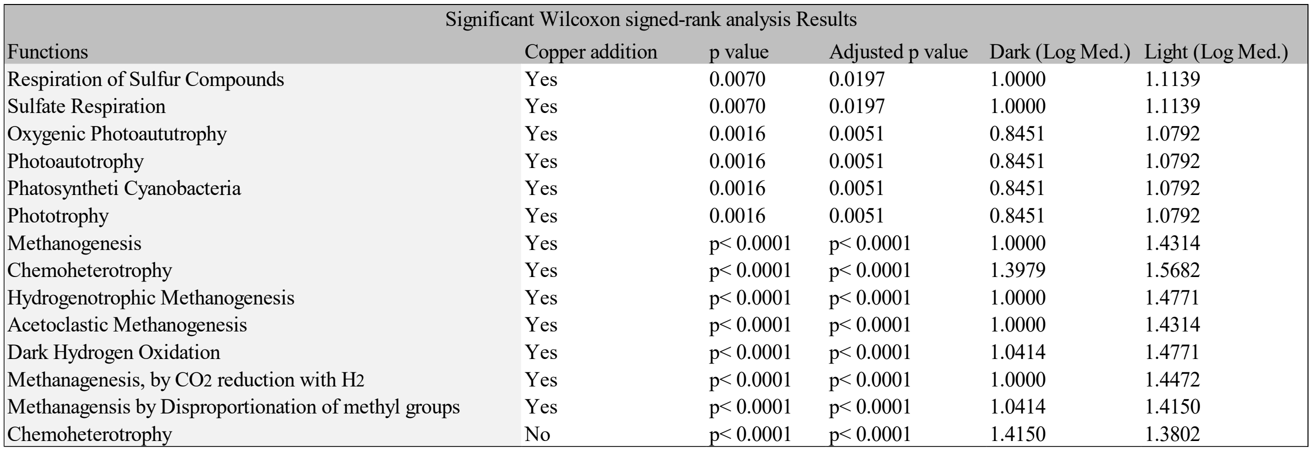

Significant Wilcoxon signed-rank analysis Results					
Functions	Copper addition	p value	Adjusted p value	Dark (Log Med.)	Light (Log Med.)
Respiration of Sulfur Compounds	Yes	0.0070	0.0197	1.0000	1.1139
Sulfate Respiration	Yes	0.0070	0.0197	1.0000	1.1139
Oxygenic Photoaututrophy	Yes	0.0016	0.0051	0.8451	1.0792
Photoautotrophy	Yes	0.0016	0.0051	0.8451	1.0792
Phatosyntheti Cyanobacteria	Yes	0.0016	0.0051	0.8451	1.0792
Phototrophy	Yes	0.0016	0.0051	0.8451	1.0792
Methanogenesis	Yes	p< 0.0001	p< 0.0001	1.0000	1.4314
Chemoheterotrophy	Yes	p< 0.0001	p< 0.0001	1.3979	1.5682
Hydrogenotrophic Methanogenesis	Yes	p< 0.0001	p< 0.0001	1.0000	1.4771
Acetoclastic Methanogenesis	Yes	p< 0.0001	p< 0.0001	1.0000	1.4314
Dark Hydrogen Oxidation	Yes	p< 0.0001	p< 0.0001	1.0414	1.4771
Methanagenesis, by CO_2 reduction with H_2	Yes	p< 0.0001	p< 0.0001	1.0000	1.4472
Methanagensis by Disproportionation of methyl groups	Yes	p< 0.0001	p< 0.0001	1.0414	1.4150
Chemoheterotrophy	No	p< 0.0001	p< 0.0001	1.4150	1.3802

*"Dark (Log Med.)" and "Light (Log Med.)" refer to the median log-transformed relative abundance of each category under dark and light conditions, respectively

Table 5. Comparison of median log-transformed relative abundances of taxonomic Orders within different functional groups between light and dark treatments.

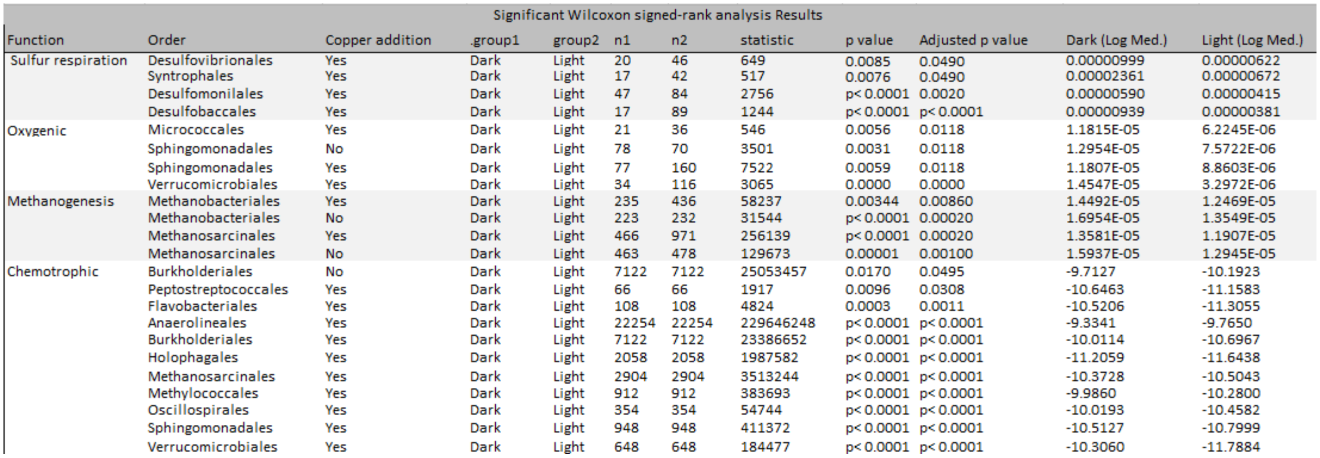

Significant Wilcoxon signed-rank analysis Results

Function	Order	Copper addition	.group1	group2	n1	n2	statistic	p value	Adjusted p value	Dark (Log Med.)	Light (Log Med.)
Sulfur respiration	Desulfovibrionales	Yes	Dark	Light	20	46	649	0.0085	0.0490	0.00000999	0.00000622
	Syntrophales	Yes	Dark	Light	17	42	517	0.0076	0.0490	0.00002361	0.00000672
	Desulfomonilales	Yes	Dark	Light	47	84	2756	p< 0.0001	0.0020	0.00000590	0.00000415
	Desulfobaccales	Yes	Dark	Light	17	89	1244	p< 0.0001	p< 0.0001	0.00000939	0.00000381
Oxygenic	Micrococcales	Yes	Dark	Light	21	36	546	0.0056	0.0118	1.1815E-05	6.2245E-06
	Sphingomonadales	No	Dark	Light	78	70	3501	0.0031	0.0118	1.2954E-05	7.5722E-06
	Sphingomonadales	Yes	Dark	Light	77	160	7522	0.0059	0.0118	1.1807E-05	8.8603E-06
	Verrucomicrobiales	Yes	Dark	Light	34	116	3065	0.0000	0.0000	1.4547E-05	3.2972E-06
Methanogenesis	Methanobacteriales	Yes	Dark	Light	235	436	58237	0.00344	0.00860	1.4492E-05	1.2469E-05
	Methanobacteriales	No	Dark	Light	223	232	31544	p< 0.0001	0.00020	1.6954E-05	1.3549E-05
	Methanosarcinales	Yes	Dark	Light	466	971	256139	p< 0.0001	0.00020	1.3581E-05	1.1907E-05
	Methanosarcinales	No	Dark	Light	463	478	129673	0.00001	0.00100	1.5937E-05	1.2945E-05
Chemotrophic	Burkholderiales	No	Dark	Light	7122	7122	25053457	0.0170	0.0495	-9.7127	-10.1923
	Peptostreptococcales	Yes	Dark	Light	66	66	1917	0.0096	0.0308	-10.6463	-11.1583
	Flavobacteriales	Yes	Dark	Light	108	108	4824	0.0003	0.0011	-10.5206	-11.3055
	Anaerolineales	Yes	Dark	Light	22254	22254	229646248	p< 0.0001	p< 0.0001	-9.3341	-9.7650
	Burkholderiales	Yes	Dark	Light	7122	7122	23386652	p< 0.0001	p< 0.0001	-10.0114	-10.6967
	Holophagales	Yes	Dark	Light	2058	2058	1987582	p< 0.0001	p< 0.0001	-11.2059	-11.6438
	Methanosarcinales	Yes	Dark	Light	2904	2904	3513244	p< 0.0001	p< 0.0001	-10.3728	-10.5043
	Methylococcales	Yes	Dark	Light	912	912	383693	p< 0.0001	p< 0.0001	-9.9860	-10.2800
	Oscillospirales	Yes	Dark	Light	354	354	54744	p< 0.0001	p< 0.0001	-10.0193	-10.4582
	Sphingomonadales	Yes	Dark	Light	948	948	411372	p< 0.0001	p< 0.0001	-10.5127	-10.7999
	Verrucomicrobiales	Yes	Dark	Light	648	648	184477	p< 0.0001	p< 0.0001	-10.3060	-11.7884

*“Dark (Log Med.)” and “Light (Log Med.)” refer to the median log-transformed abundance relative of each category under dark and light conditions, respectively.

CHAPTER 4

DISCUSSION

The fate of metals in wetland water columns plays a key role in determining the ability of these ecosystems to filter and retain pollutants. Interactions between microbial communities and abiotic factors—such as redox conditions and light availability—are critical in shaping metal mobility and bioavailability. By examining how microbial responses change with light exposure, we can better understand the biogeochemical mechanisms that govern metal cycling in wetlands. The research presented here indicates that light exposure in both natural and constructed wetlands can alter the predicted functional capacity of microbial communities, and potentially influences the partitioning of copper between the wetland water column and sediment. Specifically, light exposure has the potential to facilitate metal retention in sediment under non-copper-stressed conditions but appears to hinder retention once an elevated copper stress is introduced into the system.

I documented that sediment-to-water copper ratios in wetland-representative microcosms incubated in the field differed when exposed to natural diel cycles of light compared to those without any light exposure. A higher proportion of copper occurred in the sediment when microcosms experienced diel light cycles than only darkness; however, after four days, when an experimental spike of copper was added to microcosm water, this was reversed, and it was the dark microcosms that retained a greater proportion of copper in the sediment. These shifts in copper distribution were accompanied by changes in chlorophyll-*a* concentrations and the relative abundances of microbial orders and predicted functional groups. Most microbial taxonomic and functional differences between light and dark treatments only arose in the post copper addition group

It is important to recognize that copper distributions measured before and after metal addition correspond to distinct experimental time points, limiting direct comparison between them. For example, an alternative, time-based explanation for the observed chlorophyll-*a* pattern is that chlorophyll-*a* concentrations remained low in dark treatments due to the absence of light for photosynthesis, while initially elevated levels in light treatments declined by day eight, potentially due to secondary resource limitation of photoautotrophs.

Collectively, these results provide evidence that light exposure shapes relative abundance changes in microbial community members and potential function in wetlands, with direct consequences for copper retention. Furthermore, our findings indicate that microbial community responses to copper can shift retention patterns for this metal regardless of whether the wetland is constructed for metal removal or naturally occurring.

Abiotic Factors Pre-Copper Addition

Before a copper spike was added, the sediment-to-water copper ratio in microcosms experiencing natural diel cycles was, on average, 1.29 times higher than that of microcosms incubated only in the dark. This suggests that cyclical light exposure under pre-stress conditions facilitates metal particulate formation and/or retention in sediments more effectively than in 24-hour dark conditions. This aligns with findings by Cheloni and Slaveykova (2018), who observed that light, particularly ultraviolet radiation, can alter the structure and reactivity of dissolved organic matter, thereby increasing metal bioavailability and influencing metal uptake by photosynthetic microorganisms. Their review highlights that light-driven changes in the chemical environment and microbial responses can significantly affect trace metal dynamics in aquatic systems, depending on light intensity, spectral composition, and prior exposure conditions.

Despite increased chlorophyll-*a* concentrations and elevated relative abundances of phototrophic bacteria such as *Sphingomonadales*, dissolved oxygen levels in light treatment microcosms were, on average, lower than those constantly in the dark. This apparent paradox may suggest that enhanced heterotrophic or phototrophic activity under light conditions contributed to localized oxygen consumption, which in turn could influence redox-sensitive metal retention in sediments. For example, higher oxygen consumption may result from oxygen-respiring heterotrophs or sulfur-oxidizing phototrophs (SOP), the latter of which uses oxygen to oxidize inorganic sulfur compounds (Ljungdahl et al., 2003; Reddy & DeLaune, 2008). While not statistically backed, there is some indication of this interaction in the microcosms with patterns of SOP *Sulufritalea*, and *Sulfurisoma* within the Burkholderiales order that may have a greater relative abundance in the water of light treatment groups.

This study included both water and sediment components in the microcosms, which distinguishes it from many traditional phototrophic studies that use only water. The inclusion of sediment introduces additional complexity to oxygen dynamics and facilitates oxygen–metal–microbe interactions that may significantly influence metal cycling. Although this oxygen consumption might reduce the thickness of the oxic layer in sediments, earlier studies, such as Katano et al. (2021), demonstrated that light-driven photosynthesis can enhance sediment oxygenation by stimulating algal growth and benthic activity, resulting in a more extensive oxic zone. In this study, oxygen sensors were positioned near the bottom of the microcosms, close to the sediment surface, where this oxic–anoxic transition is expected to occur. This expanded oxic layer may facilitate abiotic binding of metals like copper to organic matter or iron/manganese oxides, thereby increasing their retention in sediments and temporarily reducing their mobility into the water column (Katano et al. 2021). Together, these findings suggest a complex interplay in which light exposure promotes both microbial oxygen consumption and oxic zone expansion, increasing iron oxide copper complex and enhancing sedimentary metal retention under pre-stress conditions.

Biotic Factors Pre-Copper Addition

Before copper addition, dark-incubated microcosms showed higher relative abundances of strict anaerobic methanogenic orders—Methanobacteriales and Methanosarcinales. These classical hydrogenotrophic and acetoclastic methanogens typically thrive in reducing environments and are known to directly compete with sulfate-reducing prokaryotes (SRPs) for substrates such as hydrogen and acetate (Lovley, 1983). Their presence implies that even under moderately oxygenated conditions in the water column, dark microcosms may have supported localized anaerobic niches within the sediment where such competition could occur. This substrate competition can suppress SRPs activity, limiting H_2S production and subsequently reducing the formation of metal sulfides that immobilize copper (Hines et al., 1989; Holmer & Nielsen, 1997). Thus, although fewer methanogens were present overall, their identity suggests a more competitive anaerobic environment for sulfur cycling, potentially influencing early-stage copper dynamics.

Post-Copper Addition: Retention Reversal and Microbial Influence

Copper can enter wetlands intermittently—such as through copper sulfate applications for algae control—or continuously, via the inflow of metal-contaminated water in constructed systems. My study demonstrates that copper additions during the experiment behave differently under light exposure, suggesting that light modifies copper dynamics in a distinct way compared to legacy contamination effects. After a copper spike was added, the sediment-to-water copper ratio of microcosms experiencing the diel light cycle decreased on average by 2.619 compared to the dark treatment, despite minimal changes in abiotic factors. These findings suggest that the retention of metal particulates under light conditions may be driven by shifts in the microbial community and their corresponding functions.

Microbial Communities Post-Copper Addition

Despite the overall functional group of sulfur reducing microbes having higher relative abundance in the light treatment group, the individual orders Desulfovibrionales and Desulfomoniales had greater relative abundance in dark microcosms after the copper addition. This is consistent with their known roles as strict anaerobes that perform classical sulfate reduction, to generate metal sulfides such as copper sulfides under low-oxygen conditions (Kuever, J, 2014, DeWeerd, Townsend, & Suflita, 2015). In contrast, Syntrophales and Desulfobaccales had higher relative abundances in the light treatments. These orders are facultative microaerophiles, groups that are more tolerant of light and oxygen exposure as seen in previous studies (Morais et al 2024, Leja K et al 2014). Unlike Desulfovibrionales and Desulfomoniales, Syntrophales and Desulfobaccales are not strictly sulfate reducers. Syntrophales undergo syntrophic fermentation that supports rather than directly creates hydrogen sulfide, and Desulfobaccales species undergo direct sulfur reduction but also can undergo aerobic respiration (Mayumi et al., 2010, Leja K et al 2014). Together, these findings suggest that light exposure restructures the composition of sulfur-respiring microbial communities, potentially shifting to less efficient sulfur reducing organisms under metal stress despite a relative overall higher functional abundance.

Phototrophic microbial taxa have been shown to play significant roles in metal cycling in aquatic environments by influencing oxygen production, shifting redox potential, and stimulating sulfur-oxidizing processes under light conditions (Ljungdahl et al., 2003). Increased photosynthetic relative abundances have been associated with enhanced oxygen production via phototrophic activity but also with the stimulation of sulfur-oxidizing phototroph (SOP) metabolism (Ljungdahl et al., 2003; Reddy & DeLaune, 2008). My findings support this, as Sphingomonadales—as well as other photoactive orders such as Micrococcales and Verrucomicrobiales—exhibited significantly higher relative abundance in the light treatment compared to the dark following copper addition. Higher SOP activity would have the potential to increase hydrogen sulfide (H_2S) oxidation, reducing its availability for reactions with copper to create copper sulfide. Notably, all three of these bacterial orders were also classified within cyanobacterial-associated functional groups, which may contribute to increased system toxicity through the production of reactive oxygen species or secondary metabolites, potentially inhibiting the growth and activity of sulfate-reducing bacteria and other sensitive anaerobes (Savadova-Ratkus et al., 2021).

When I artificially elevated the copper concentration of microcosms, several chemoorganotrophic and facultative anaerobic bacterial orders—including Anaerolineales, and Holophagales—had higher relative abundances in dark treatments compared to light. All identified groups are adapted to low-oxygen or anaerobic environments and are often involved in complex organic matter degradation through fermentative or syntrophic pathways (Fukunaga & Ichikawa, 2014; Petriglieri et al., 2023; Fischbach & Sonnenburg, 2011; Park et al., 2016, Nikitina et al., 2023; Lee et al., 2011). Their enrichment under dark conditions aligns with the suppression of phototroph-mediated oxygenation, creating favorable conditions for anaerobic respiration processes. Several of these orders—particularly, Anaerolineales, and Holophagales—are known to participate in sulfide production either directly or through cross-feeding with sulfate-reducing bacteria, thereby contributing to hydrogen sulfide (H_2S) accumulation in sediments (Lee et al., 2011, Wasmund et al.,2017, Kielak et al. 2016). This microbial structure likely supports SRPs metabolic activity by supplying substrates such as acetate or hydrogen, which are critical for dissimilatory sulfate reduction. Such metabolic support can enhance the competitive advantage of SRPs over methanogens, which rely on similar substrates (Lovley & Klug, 1983).

Methanogens, through their interactions and competition with sulfate-reducing prokaryotes, can play a key indirect role in shaping copper dynamics in sediment environments. After copper addition, total methanogen relative abundance was significantly higher in light-exposed microcosms. While specific taxonomic identities varied, their expansion in light treatments suggests an increase in competition with SRPs within this treatment group when compared to dark microcosms. This shift could suppress classical sulfate reduction, lower H_2S concentrations, and decreasing copper sulfide formation. The result: less copper retention in sediments and higher dissolved copper levels in the light-exposed systems. These findings are reinforced by previous researched descriptions of competitive dynamics with SRPs and methanogenesis species (Lovley, 1983; Hines et al., 1989; Holmer & Nielsen, 1997).

The lower relative counts of methanogens in light treatments suggest that increased oxygen availability and sulfur-oxidizing phototrophic (SOP) activity may suppress anaerobic fermenters and SRPs-supporting consortia. Thus, their presence in the dark treatment not only reinforces the potential for anaerobic conditions but may also indirectly promote metal immobilization through enhanced sulfide production and reductive dissolution mechanisms. This would agree with the greater delivery and retention of copper in the sediment that I found for dark-only microcosms compared to light-exposed microcosms when both treatments spiked with copper.

Microbial Community Richness and Evenness

Despite no detectable differences in the beta diversity of microbial communities, alpha diversity differed between light-exposed and dark-only microcosms in both pre and post copper additions When microbial communities were restricted to complete darkness, they exhibited higher evenness but lower richness, suggesting that while there are a number of microbial taxa present, fewer, highly abundant groups may dominate the community. Communities with high evenness and low richness may reflect a more stable or uniform environment, where certain anaerobic specialists thrive and outcompete others, leading to dominance (Chesson, 2000). Alternatively, this pattern could arise in systems with fewer overall niches, but where each niche is more isolated, allowing specialized taxa to flourish independently with minimal competition or overlap (Chesson, 2000). In contrast, light treatments had lower evenness but higher richness, indicating that while fewer organisms are present in each species overall, there is a higher number of species present. This may suggest a more variable or heterogeneous environment, where phototrophic activity, oxygen gradients, and light-driven dynamics create a greater number of viable ecological niches, promoting coexistence without dominance.

These differences in community structure may influence how microbial communities respond to stressors such as copper. In dark treatments, where evenness was higher, additional copper exposure led to increased metal retention in sediment compared to pre-stress conditions. One explanation is that when dominant taxa were impacted by copper, less abundant but potentially metal-tolerant taxa or those that rely on copper for their enzyme function were able to occupy available niches and maintain or even enhance functional processes like metal retention. For example, Desulfovibrionales and Desulfomoniales show a more prominent role in these communities. This highlights a potential "insurance effect" of richness—greater taxonomic diversity provides more opportunities for functional compensation under stress (Yachi & Loreau, 1999).

Conversely, in light treatments, where richness was higher, metal retention decreased following copper exposure. The richer but less even communities may lack the functional redundancy needed to maintain performance when key taxa are lost due to metal toxicity, leading to a loss of function under stress. Thus, while light-exposed communities may be better adapted to dynamic environments under normal conditions, they may be more vulnerable to novel stressors that disrupt specific functional groups. This is supported by previous studies like Cheloni and Slaveykova (2018) which found that trace metals disproportionately affect photosynthetic microbial groups under light conditions, supporting the idea that disruptions to specific functional groups lead to loss of function.

Comparison of Sarracenia Bay and H-02 Wetlands

We observed differences in chlorophyll-*a*, ortho-phosphate and copper sediment-to-water ratios between Sarracenia Bay and H-02 microcosms despite the lack of significant differences between microbial communities, and all other abiotic factors measured. These observations may be partially explained by vegetation legacy effects and site-specific contamination histories.

Sarracenia Bay is dominated primary by *Nymphaea odorata* (American white-water lily), that allows greater light penetration into the water column compared to the dense surface mats formed by *Lemna minor* (duckweed) and *Schoenoplectus californicus* (bulrushes) that is the primary foliage in H-02. Increased light availability under *N. odorata* can support greater phytoplankton productivity, consistent with the elevated chlorophyll-*a* concentrations observed in Sarracenia Bay microcosms. It is possible that plant coverage like *Nymphaea* can promote algal growth by allowing sufficient light transmission, in contrast to duckweed, which significantly suppresses it through dense shading (Barko & Smart, 1981; Van Nes et al., 2002). This could lead to increased algal photosynthesis and benthic microbial activity, leading to a thicker oxic layer that more effectively binds copper and limits its release into overlying water abiotically (Katano et al. 2021).

The H-02 wetland plants *L. minor* and *S. californicus* are known for their nutrient uptake and metal retention capabilities, particularly nitrate, phosphate, and heavy metals such as copper (Tanner, 2001; Akratos & Tsihrintzis, 2007, Harguinteguy, Arán, Gudiño, & Peñaflor, 2023). However, these active remediation pathways are absent in this experiment's microcosms, leaving only the legacy of environmental conditioning (e.g., sediment chemistry and microbial composition). This vegetation-driven history shaped the biogeochemical context of each wetland, influencing sediment oxygenation and copper-binding potential even without live plant uptake shifting the base lines of wetland microcosms.

Given the lack of significant differences in microbial community composition and most other abiotic factors, our results suggest that both wetlands, despite differences in location and contamination levels, exhibited similar microbial responses and potential for functional resilience to metal stress and its interaction with light. This pattern aligns with findings from

Gilbert, Fulthorpe, and Kirkwood (2012), who reported high similarity in sediment microbial community composition and function across urban wetlands in Ontario, Canada. Despite differing contaminant input regimes and exposure histories, microbial communities in their study exhibited overlapping diversity profiles and functional characteristics. Given that many of the taxa identified in my study are also sediment-associated, these results support the idea that wetland microbial assemblages may possess inherent resilience and functional redundancy, allowing them to maintain similar community structure and activity under varying environmental pressures.

Experimental Limitations

Several considerations should be made when interpreting our findings. The work was conducted with a smaller size of 34 microcosms and is based around two wetland sources, one a constructed wetland and another a naturally occurring Carolina Bay both located in the southeastern United States. Due to the limitation of both experimental scale and sampling locations, results may not be broadly generalized across wetland categories or geographic regions. For example, dissolved oxygen may have been depleted much faster in the enclosed microcosms than in the real wetland, due to the closed system experimental set up. Similarly, Reddy and DeLaune (2008) demonstrated that microbial responses to metal inputs, such as copper, can vary significantly depending on wetland type by examining biogeochemical processes in saltwater marshes, which experience tidal flushing and elevated salinity.

It is important to acknowledge the timing of sample collection relative to metal addition. In this study, samples were collected four days apart, which limits the ability to directly compare microbial community changes before and after metal exposure. Microbial communities can naturally fluctuate over short timescales due to environmental variability and ecological succession (Moxon & Kussell, 2017). Therefore, some of the taxonomic shifts observed following the metal spike might reflect natural temporal variation rather than a direct response to metal addition.

One should also consider sediment sampling depth and spatial design may have influenced observed microbial communities and metal dynamics. Although sediment was collected to a uniform depth, the selected depth encompassed microenvironments with differing redox conditions and contamination histories that were then homogenized. For instance, the upper layers of H-02 may be less contaminated than deeper sediments due to ongoing burial of legacy contamination, resulting in microbial communities that reflect a mixture of sediment layers. Studies have shown that microbial communities, such as sulfate-reducing microorganisms, shift significantly with depth, particularly across boundaries between bioturbated surface layers and deeper, unmixed sediments (Jochum et al., 2017). The disturbance of these vertical gradients in community structure could influence copper cycling and microbial responses and should be considered when applying the results to wetland ecosystems.

To address the acknowledged limitation regarding Zn background contamination, it is important to consider its potential biogeochemical interactions with both copper and microbial communities in wetland environments. Zinc, like Cu, is a transitional metal that can compete for binding sites on organic matter, sulfide minerals, and microbial cell surfaces. This competitive behavior may influence the speciation, mobility, and bioavailability of both metals (Xu and Mills, 2018). In sulfate-reducing environments, for example, Zn can also form insoluble zinc sulfides, potentially altering the availability of sulfide for Cu precipitation and thereby affecting Cu retention in sediments. Moreover, microbial communities—particularly sulfate-reducing and sulfur-oxidizing prokaryotes—may exhibit metal-specific tolerances or sensitivities, with some taxa being inhibited by Zn at lower concentrations than Cu. This could result in shifts in microbial community structure or function that confound interpretations based solely on Cu treatments. Future studies should quantify and control Zn concentrations more rigorously and explore co-metal or multi-metal interactions explicitly to disentangle their individual and synergistic effects on microbial metal cycling and environmental factors.

Broad Impacts

My findings suggest that light-driven shifts in the relative abundances of some taxonomic members of the microbial community could significantly affect a wetland's capacity to retain or transform copper, particularly under environmentally stressful conditions. By identifying phototrophic microbial groups associated with increased metal transformation or potential toxicity, this study contributes to a mechanistic understanding of contaminant fate in wetland ecosystems. These insights emphasize the importance of integrating larger scale impacts such as foliage coverage and microbial responses, especially those mediated by light availability—into the design, management, and restoration of constructed wetlands. As climate change continues to reshape aquatic systems, understanding the microbial drivers of metal cycling is critical for maintaining water quality and ecosystem health.

REFERENCES

Akratos, C. S., & Tsihrintzis, V. A. (2007). Effect of temperature, HRT, vegetation and porous \ media on removal efficiency of pilot-scale horizontal subsurface flow constructed wetlands. Ecological Engineering, 29(2), 173–191. https://doi.org/10.1016/j.ecoleng.2006.06.013

Anderson, M. J. (2017). Permutational multivariate analysis of variance (PERMANOVA). Wiley StatsRef: Statistics Reference Online, 1–15. https://doi.org/10.1002/9781118445112.stat07841

Balkcom, G., Touchstone, T., Kammermeyer, K., Vansant, V., Martin, C., Van Brackle, M., Steele, G., & Bowers, J. (2000). Waterfowl management in Georgia: Preface & acknowledgments. https://gastateparks.org/altamaha-wma

Barko, J. W., & Smart, R. M. (1981). Comparative influences of light and temperature on the growth and metabolism of selected submersed freshwater macrophytes. Ecological Monographs, 51(2), 219–235. https://doi.org/10.2307/2937264

Bates, D., Mächler, M., Bolker, B., & Walker, S. (2015). Fitting linear mixed-effects models using lme4. Journal of Statistical Software, 67(1), 1–48. https://doi.org/10.18637/jss.v067.i01

Cavalletti, E., Romano, G., Palma Esposito, F., Barra, L., Chiaiese, P., Balzano, S., & Sardo, A. (2022). Copper effect on microalgae: Toxicity and bioremediation strategies. Toxics, 10(9), 527. https://doi.org/10.3390/toxics10090527

Chesson, P. (2000). Mechanisms of maintenance of species diversity. Annual Review of Ecology and Systematics, 31, 343–366. https://doi.org/10.1146/annurev.ecolsys.31.1.343

Cheloni, G., & Slaveykova, V. I. (2018). Combined effects of trace metals and light on photosynthetic microorganisms in aquatic environment. Environments, 5(7), 81. https://doi.org/10.3390/environments5070081

Christensen, T. H., Bjerg, P. L., Banwart, S. A., Jakobsen, R., Heron, G., & Albrechtsen, H. J. (2000). Characterization of redox conditions in groundwater contaminant plumes. Journal of Contaminant Hydrology, 45,165–241. https://doi.org/10.1016/S0169-7722(00)00109-1

DeWeerd, K. A., Townsend, G. T., & Suflita, J. M. (2015). Desulfomonile. In Bergey's Manual of Systematics of Archaea and Bacteria. John Wiley & Sons. https://doi.org/10.1002/9781118960608.gbm01062

Dedysh, S. N., & Yilmaz, P. (2018). Refining the taxonomic structure of the phylum Acidobacteria. International Journal of Systematic and Evolutionary Microbiology, 68(12), 3796–3806.

Eger, P. (1994). Wetland treatment for trace metal removal from mine drainage: The importance of aerobic and anaerobic processes. Water Science and Technology, 29(12), 249-256. https://doi.org/10.2166/wst.1994.0203

Fischbach, M. A., & Sonnenburg, J. L. (2011). Eating for two: How metabolism establishes interspecies interactions in the gut. Cell Host & Microbe, 10(4), 336–347. https://doi.org/10.1016/j.chom.2011.10.002

Franson JC, Lahner LL, Meteyer CU, Rattner BA. Copper pellets simulating oral exposure to copper ammunition: absence of toxicity in American kestrels (Falco sparverius). Arch Environ Contam Toxicol. 2012;62(1):145-53. doi: 10.1007/s00244-011-9671-1. Epub 2011 Apr 22. PMID: 21512804.

Fukunaga, Y., & Ichikawa, N. (2014). The Class Holophagaceae. In E. Rosenberg, E. F. DeLong, S. Lory, E. Stackebrandt, & F. Thompson (Eds.), The Prokaryotes: Other Major Lineages of Bacteria and The Archaea (pp. 683–687). Springer. https://doi.org/10.1007/978-3-642-38954-2_161

Gilbert, N., Fulthorpe, R., & Kirkwood, A. E. (2012). Microbial diversity, tolerance, and biodegradation potential of urban wetlands with different input regimes. Canadian Journal of Microbiology, 58(9), 1115–1124. https://doi.org/10.1139/w2012-066

Harguinteguy, C. A., Arán, D. S., Gudiño, G. L., & Peñaflor, M. (2023). Capacity of *Schoenoplectus californicus* to remove and tolerate copper, lead, and zinc in constructed wetland systems using simulated wastewater. *Journal of Environmental Engineering, 149*(10). https://doi.org/10.1061/JOEEDU.EEENG-7334

Holmer, M., & Nielsen, S. L. (1997). Sediment sulfur dynamics related to biomass-density patterns in Zostera marina (eelgrass) beds. Marine Ecology Progress Series, 146(1/3), 163–171. http://www.jstor.org/stable/24857450

Hu, S., Niu, Z., Chen, Y., Li, L., & Zhang, H. (2017). Global wetlands: Potential distribution, wetland loss, and status. Science of the Total Environment, 586, 319–327. https://doi.org/10.1016/j.scitotenv.2017.02.001

Jochum, L. M., Chen, X., Lever, M. A., Loy, A., Jørgensen, B. B., Schramm, A., & Kjeldsen, K. U. (2017). Depth distribution and assembly of sulfate-reducing microbial communities in marine sediments of Aarhus Bay. Applied and Environmental Microbiology, 83(23), e01547-17. https://doi.org/10.1128/AEM.01547-17

Kang, M., Tian, Y., Peng, S., & Wang, M. (2019). Effect of dissolved oxygen and nutrient levels on heavy metal contents and fractions in river surface sediments. Science of The Total Environment, 648, 861–870. https://doi.org/10.1016/j.scitotenv.2018.08.201

Katano, T., Watanabe, K., Ohgaki, H., et al. (2021). Light-induced changes in oxygen conditions and metal/nutrient release in lake sediments. Science of the Total Environment, 756, 144030. https://doi.org/10.1016/j.scitotenv.2020.144030

Kielak, A. M., Barreto, C. C., Kowalchuk, G. A., van Veen, J. A., & Kuramae, E. E. (2016). The ecology of Acidobacteria: Moving beyond genes and genomes. Frontiers in Microbiology, 7, 744. https://doi.org/10.3389/fmicb.2016.00744

Kohler, T.J., S. Fodelianakis, G. Michoud, L. Ezzat, et al. 2022. Glacier shrinkage will accelerate downstream decomposition of organic matter and alters microbiome structure and function. Global Change Biology 28:3846–3859.

Kuever, J. (2014). The Family Desulfovibrionaceae. In: Rosenberg, E., DeLong, E.F., Lory, S., Stackebrandt, E., Thompson, F. (eds) The Prokaryotes. Springer, Berlin, Heidelberg. https://doi.org/10.1007/978-3-642-39044-9_272

Ladomersky, E., & Petris, M. J. (2015). Copper tolerance and virulence in bacteria. Metallomics, 7(6), 957–964. https://doi.org/10.1039/c4mt00327f

Lahti, L., & Shetty, S. (2012–2019). microbiome R package (Version 1.19.1) [Computer software]. https://microbiome.github.io

Lee, K. C.-Y., Dunfield, P. F., Morgan, X. C., Crowe, M. A., Houghton, K. M., Vyssotski, M., Ryan, J. L. J., Lagutin, K., McDonald, I. R., & Stott, M. B. (2011). Chthonomonas calidirosea gen. nov., sp. nov., an aerobic, saccharolytic, moderately thermophilic bacterium of the newly described phylum Armatimonadetes. International Journal of Systematic and Evolutionary Microbiology, 61(11), 2658–2666. https://doi.org/10.1099/ijs.0.025502-0

Leja, K., Myszka, K., Olkowicz, M., Juzwa, W., & Czaczyk, K. (2014). Clostridium bifermentans as an aero-tolerant exponent of strictly anaerobe genera. Advances in Microbiology, 4(4), 273–281. https://doi.org/10.4236/aim.2014.44028

Liu, X., Huo, P., Wang, W., Li, D., Zeng, G., & Lyu, S. (2023). Simultaneous immobilization of heavy metals and nutrient elements in contaminated sediment using a novel composite agent product. Water Science and Technology, 88(1), 288–299. https://doi.org/10.2166/wst.2023.216

Ljungdahl, L. G., Adams, M. W., Barton, L., Ferry, J. G., & Johnson, M. K. (Eds.). (2003). Biochemistry and physiology of anaerobic bacteria. Springer Science & Business Media. https://doi.org/10.1007/b98857

Lovley, D. R., & Klug, M. J. (1983). Sulfate reducers can outcompete methanogens at freshwater sulfate concentrations. Applied and Environmental Microbiology, 45(1), 187–192. https://doi.org/10.1128/aem.45.1.187-192.1983

Lytle, D. A., Schock, M. R., Leo, J., & Barnes, B. (2018). A model for estimating the impact of orthophosphate on copper in water. Journal of the American Water Works Association, 110(10), E1–E15. https://doi.org/10.1002/awwa.1109

Norris, J. R., Allen, R. J., Evan, A. T., Zelinka, M. D., O’Dell, C. W., & Klein, S. A. (2016). Evidence for climate change in the satellite cloud record. Nature, 536, 72–75. https://doi.org/10.1038/nature18273

Mayumi, D., Mochimaru, H., Yoshioka, H., Sakata, S., Maeda, H., Miyagawa, Y., Ikarashi, M., Takeuchi, M., & Kamagata, Y. (2010). Evidence for syntrophic acetate oxidation coupled to hydrogenotrophic methanogenesis in the high-temperature petroleum reservoir of Yabase oil field (Japan). Environmental Microbiology, 13(8), 1995–2006. https://doi.org/10.1111/j.1462-2920.2010.02338.x

McMurdie, P. J., & Holmes, S. (2013). phyloseq: An R package for reproducible interactive analysis and graphics of microbiome census data. PLOS ONE, 8(4), e61217. https://doi.org/10.1371/journal.pone.0061217

Morais, B. P., Magalhães, C. P., Martins, G., et al. (2024). Effect of micro-aeration on syntrophic and methanogenic activity in anaerobic sludge. Applied Microbiology and Biotechnology, 108, 192. https://doi.org/10.1007/s00253-023-12969-4

Moxon, R., & Kussell, E. (2017). The impact of bottlenecks on microbial survival, adaptation and phenotypic switching in host-pathogen interactions. Evolution, 71(12), 2803–2816. https://doi.org/10.1111/evo.13370

Mulderij, G., Van Nes, E. H., & Van Donk, E. (2007). Macrophyte–phytoplankton interactions:

The relative importance of allelopathy versus other factors. Ecological Modelling, 204(1-2). https://doi.org/10.1016/j.ecolmodel.2006.12.020

Nikitina, A. A., Kallistova, A. Y., Grouzdev, D. S., Kolganova, T. V., Kovalev, A. A., Kovalev, D. A., Panchenko, V., Zekker, I., Nozhevnikova, A. N., & Litti, Y. V. (2023). Syntrophic butyrate-oxidizing consortium mitigates acetate inhibition through a shift from acetoclastic to hydrogenotrophic methanogenesis and alleviates VFA stress in thermophilic anaerobic digestion. Applied Sciences, 13(1), 173. https://doi.org/10.3390/app13010173

Oksanen, J., Blanchet, F. G., Friendly, M., et al. (2022). vegan: Community Ecology Package. R package version 2.6-4. https://CRAN.R-project.org/package=vegan

Oksanen, J., Simpson, G. L., Blanchet, F. G., Kindt, R., Legendre, P., Minchin, P. R., O'Hara, R. B., Solymos, P., Stevens, M. H. H., Szoecs, E., Wagner, H., Barbour, M., Bedward, M., Bolker, B., Borcard, D., Borman, T., Carvalho, G., Chirico, M., De Cáceres, M., ... Weedon, J. (2025). vegan: Community Ecology Package (Version 2.7-0) [R package]. https://vegandevs.github.io/vegan/

Park, G., Takekawa, M., Soda, S., Ike, M., & Furukawa, K. (2016). Temperature dependence of nitrogen removal activity by anammox bacteria enriched at low temperatures. Journal of Bioscience and Bioengineering, 123(4), 483–489. https://doi.org/10.1016/j.jbiosc.2016.11.009

Paulson JN, Olson ND, Braccia DJ, Wagner J, Talukder H, Pop M, Bravo HC (2013). metagenomeSeq: Statistical analysis for sparse high-throughput sequncing.. Bioconductor package, http://www.cbcb.umd.edu/software/metagenomeSeq.

Petriglieri, F., Kondrotaite, Z., Singleton, C., Nierychlo, M., Dueholm, M. K. D., & Nielsen, P. H. (2023). A comprehensive overview of the Chloroflexota community in wastewater treatment plants worldwide. mSystems, 8(6), e00667-23. https://doi.org/10.1128/msystems.00667-23

Rahimzadeh, M. R., Rahimzadeh, M. R., Kazemi, S., & Moghadamnia, A. A. (2024). Copper poisoning with emphasis on its clinical manifestations and treatment of intoxication. Advances in Public Health, 2024, Article 6001014. https://doi.org/10.1155/2024/6001014

R Core Team. (2023). R: A language and environment for statistical computing. R Foundation for Statistical Computing, Vienna, Austria. https://www.R-project.org/

Reddy, K. R., & DeLaune, R. D. (2008). Biogeochemistry of wetlands: Science and applications (1st ed.). CRC Press. https://doi.org/10.1201/9780203491454

Rensing, C., & Grass, G. (2003). Escherichia coli mechanisms of copper homeostasis in a changing environment. FEMS Microbiology Reviews, 27(2-3), 197–213. https://doi.org/10.1016/S0168-6445(03)00049-4

Richard, F. J., Southern, I., Gigauri, M., Bellini, G., Rojas, O., & Runde, A. (2021). Warning on nine pollutants and their effects on avian communities. Global Ecology and Conservation, 28, e01898. https://doi.org/10.1016/j.gecco.2021.e01898

Rosemond, A. D., Benstead, J. P., Bumpers, P. M., Gulis, V., Kominoski, J. S., Manning, D. W. P., Suberkropp, K., & Wallace, J. B. (2015). Experimental nutrient additions accelerate terrestrial carbon loss from stream ecosystems. Science, 347(6226), 1142–1145. https://doi.org/10.1126/science.aaa1958

Savadova-Ratkus, K., Mazur-Marzec, H., Karosienė, J., Kasperovičienė, J., Paškauskas, R., Vitonytė, I., & Koreivienė, J. (2021). Interplay of nutrients, temperature, and competition of native and alien cyanobacteria species growth and cyanotoxin production in temperate lakes. Toxins, 13(1), 23. https://doi.org/10.3390/toxins13010023

Tanner C. C. (2001). Plants as ecosystem engineers in subsurface-flow treatment wetlands. Water science and technology : a journal of the International Association on Water Pollution Research, 44(11-12), 9–17. https://doi.org/10.2166/wst.2001.0804

Tipping, E. (2002). Cation binding by humic substances. Cambridge University Press. https://doi.org/10.1017/CBO9780511535741

Trevors, J. T., & Cotter, C. M. (1990). Copper toxicity and uptake in microorganisms. Journal of Industrial Microbiology, 6(2), 77–84. https://doi.org/10.1007/BF01576426

Vymazal, J. (2011). Plants used in constructed wetlands with horizontal subsurface flow: A review. Hydrobiologia, 674, 133–156. https://doi.org/10.1007/s10750-011-0738-9

Vymazal, J. (2014). Constructed wetlands for treatment of industrial wastewaters: A review. Ecological Engineering, 73, 724–751. https://doi.org/10.1016/j.ecoleng.2014.09.034

Wasmund, K., Mußmann, M., & Loy, A. (2017). The life sulfuric: Microbial ecology of sulfur cycling in marine sediments. Environmental Microbiology Reports, 9(4), 323–344. https://doi.org/10.1111/1758-2229.12538

Wilson, B., & Pyatt, F. B. (2007). Heavy metal dispersion, persistence, and bioaccumulation around an ancient copper mine situated in Anglesey, UK. Ecotoxicology and Environmental Safety, 66(2), 224–231. https://doi.org/10.1016/j.ecoenv.2006.02.015

Wintermans, J. F. G. M., & De Mots, A. (1965). Spectrophotometric characteristics of chlorophylls a and b and their phenophytins in ethanol. Biochimica et Biophysica Acta, 109, 448–453. https://doi.org/10.1016/0926-6585(65)90170-6

Xu, X., & Mills, G. L. (2018). Do constructed wetlands remove metals or increase metal bioavailability? Journal of Environmental Management, 213, 245–255. https://doi.org/10.1016/j.jenvman.2018.04.014

Yachi, S., & Loreau, M. (1999). Biodiversity and ecosystem productivity in a fluctuating environment: The insurance hypothesis. Proceedings of the National Academy of Sciences, 96(4), 1463–1468. https://doi.org/10.1073/pnas.96.4.1463

Zhang, Y., Naafs, B. D. A., Huang, X., Song, Q., Xue, J., Wang, R., Zhao, M., Evershed, R. P., Pancost, R. D., & Xie, S. (2022). Variations in wetland hydrology drive rapid changes in the microbial community, carbon metabolic activity, and greenhouse gas fluxes. Geochimica et Cosmochimica Acta, 318, 14–27. https://doi.org/10.1016/j.gca.2021.11.014

Zhang, Z., Zhang, C., Yang, Y., Zhang, Z., Tang, Y., Su, P., & Lin, Z. (2022). A review of sulfate-reducing bacteria: Metabolism, influencing factors and application in wastewater treatment. Journal of Cleaner Production, 376, 134109. https://doi.org/10.1016/j.jclepro.2022.134109

APPENDIX 1

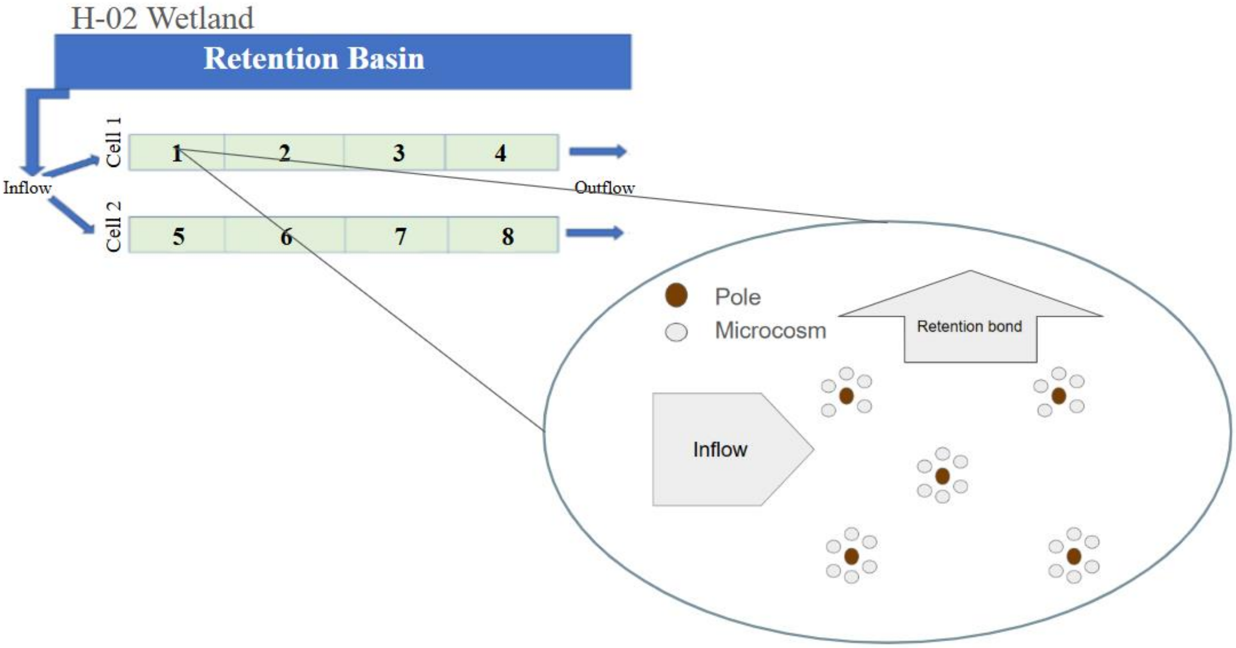

Appendix 1. Microcosm placement at the H-02 wetland. Bottle locations were chosen at random from the locations illustrated above

APPENDIX 2

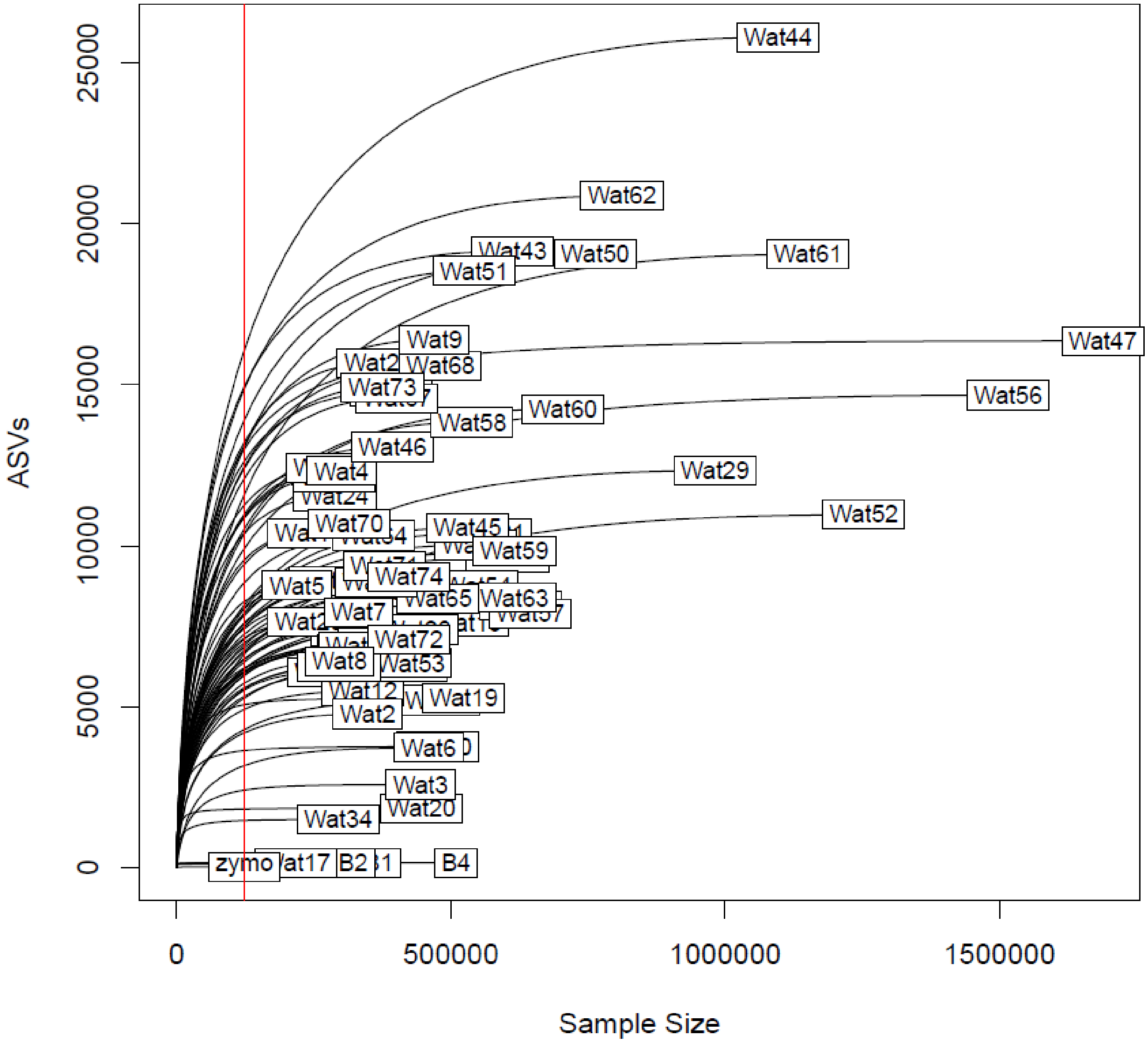

Appendix 2. Sequencing rarefaction curve to assess depth. Wat#, B#, represents individual unique identification numbers and zymo is the sequencing control community. The red line represents the alpha diversity cutoff for refraction.

APPENDIX 3

Appendix 3. Summary of linear model outputs predicting log-transformed chlorophyll-*a* concentration (log [Chl-a], μg/L)

Predictor	**Estimate**	**SE**	***t* value**	***p*-value**	**Significance**
(Intercept)	1.696	0.158	10.76	1.63×10^{-13}	***
Light Treatment (Light)	0.696	0.209	3.34	0.0018	**
Copper addition	0.048	0.198	0.24	0.8099	
Wetland Source (Sarracenia Bay)	0.468	0.144	3.25	0.0023	**
Light × Metal Interaction	–0.717	0.288	–2.49	0.0168	*

*Model fit statistics: Adjusted $R^2 = 0.345$, $F(4,41) = 6.93$, $p = 0.00023$; Residual SE = 0.486. Marginal $R^2 = 0.381$ (conditional $R^2 = 0.381$).

APPENDIX 4

Appendix 4. Summary of linear model evaluating the interactive effects of light treatment, copper addition, and wetland source on the copper sediment-to-water ratio during experimental incubations

Predictor	**Estimate**	**SE**	***t* value**	***p*-value**	**Significance**
(Intercept)	0.650	0.179	3.29	0.036	*
Light Treatment (Light)	1.294	0.227	5.71	0.0107	*
Copper addition	1.199	0.227	5.29	0.0132	*
Wetland Source (Sarracenia Bay)	0.941	0.160	5.87	0.0099	**
Light × Metal Interaction	–2.619	0.321	-8.173	0.0038	**

*Model fit statistics: Adjusted $R^2 = 0.933$, $F(4,41) = 6.93$, $p = 0.00023$; Residual SE = 0.9714. Marginal $R^2 = 0.936$ (conditional $R^2 = 0.936$). Residual standard error: 0.2266 on 3 degrees of freedom.

APPENDIX 5

Appendix 5. Chi-squared test results for the relationship between environmental variables and light treatment conditions

Variable	Chi-squared	df	p-value
Precent Dissolved Oxygen	1.8651	1	0.172
pH	0.39614	1	0.5291
Nitrate mg/l	2.0483	1	0.152
Ortho-Phosphate mg/l	7.1848	1	0.00735
hpa	0.0728	1	0.2870
Chlorophyll -*a* (µg/L)	5.2376	1	0.0221
Total Dissolved Carbon mg/l	0.09375	1	0.3329

APPENDIX 6

Appendix 6: Non-significant comparisons of median log-transformed Orders category abundance between light and dark treatments

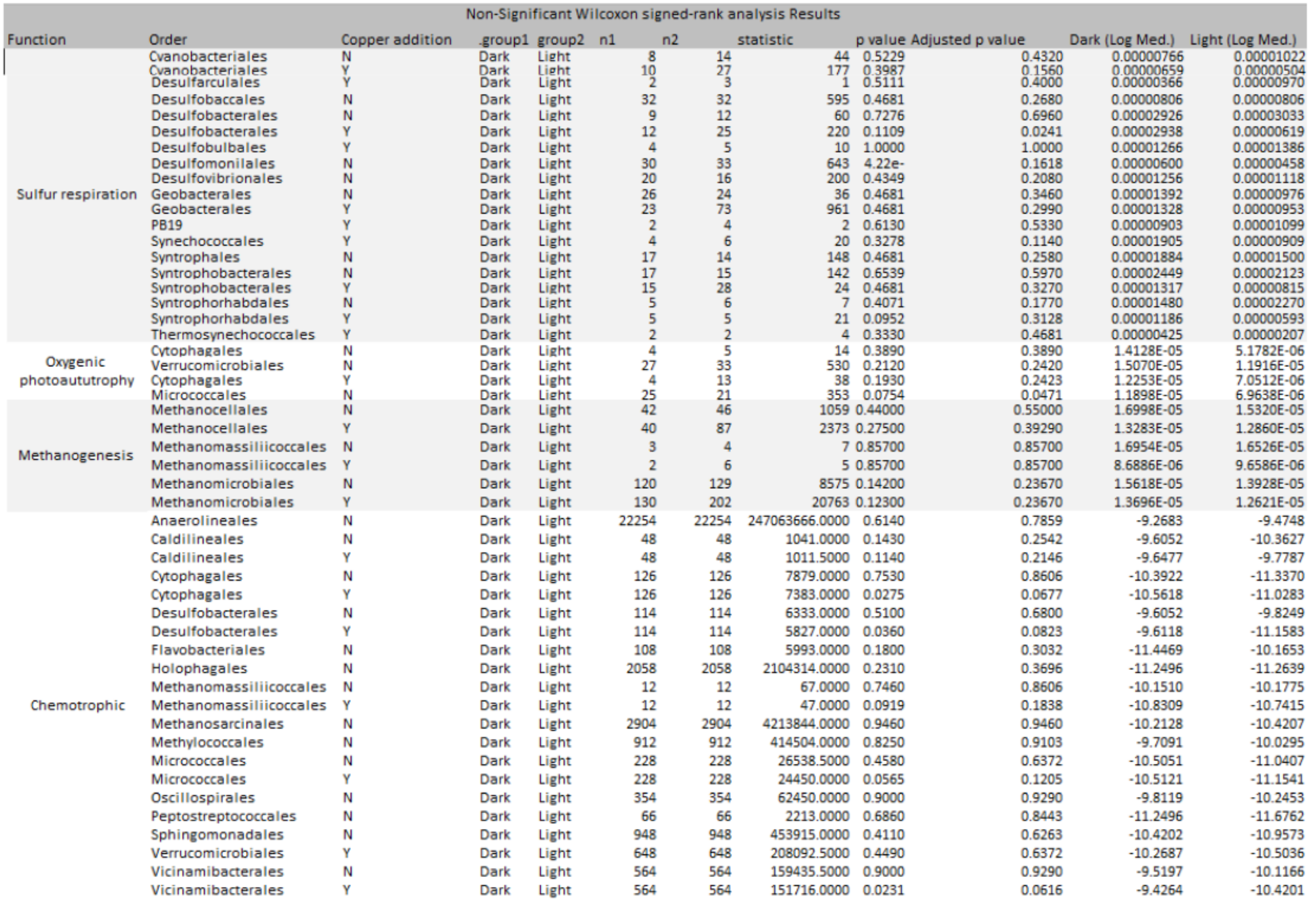

Non-Significant Wilcoxon signed-rank analysis Results

Function	Order	Copper addition	.group1	group2	n1	n2	statistic	p value	Adjusted p value	Dark (Log Med.)	Light (Log Med.)
Sulfur respiration	Cvanobacteriales	N	Dark	Light	8	14	44	0.5229	0.4320	0.00000766	0.00001022
	Cvanobacteriales	Y	Dark	Light	10	27	177	0.3987	0.1560	0.00000659	0.00000504
	Desulfarculales	Y	Dark	Light	2	3	1	0.5111	0.4000	0.00000366	0.00000970
	Desulfobaccales	N	Dark	Light	32	32	595	0.4681	0.2680	0.00000806	0.00000806
	Desulfobacterales	N	Dark	Light	9	12	60	0.7276	0.6960	0.00002926	0.00003033
	Desulfobacterales	Y	Dark	Light	12	25	220	0.1109	0.0241	0.00002938	0.00000619
	Desulfobulbales	Y	Dark	Light	4	5	10	1.0000	1.0000	0.00001266	0.00001386
	Desulfomonilales	N	Dark	Light	30	33	643	4.22e-	0.1618	0.00000600	0.00000458
	Desulfovibrionales	N	Dark	Light	20	16	200	0.4349	0.2080	0.00001256	0.00001118
	Geobacterales	N	Dark	Light	26	24	36	0.4681	0.3460	0.00001392	0.00000976
	Geobacterales	Y	Dark	Light	23	73	961	0.4681	0.2990	0.00001328	0.00000953
	PB19	Y	Dark	Light	2	4	2	0.6130	0.5330	0.00000903	0.00001099
	Synechococcales	Y	Dark	Light	4	6	20	0.3278	0.1140	0.00001905	0.00000909
	Syntrophales	N	Dark	Light	17	14	148	0.4681	0.2580	0.00001884	0.00001500
	Syntrophobacterales	N	Dark	Light	17	15	142	0.6539	0.5970	0.00002449	0.00002123
	Syntrophobacterales	Y	Dark	Light	15	28	24	0.4681	0.3270	0.00001317	0.00000815
	Syntrophorhabdales	N	Dark	Light	5	6	7	0.4071	0.1770	0.00001480	0.00002270
	Syntrophorhabdales	Y	Dark	Light	5	5	21	0.0952	0.3128	0.00001186	0.00000593
	Thermosynechococcales	Y	Dark	Light	2	2	4	0.3330	0.4681	0.00000425	0.00000207
Oxygenic photoaututrophy	Cytophagales	N	Dark	Light	4	5	14	0.3890	0.3890	1.4128E-05	5.1782E-06
	Verrucomicrobiales	N	Dark	Light	27	33	530	0.2120	0.2420	1.5070E-05	1.1916E-05
	Cytophagales	Y	Dark	Light	4	13	38	0.1930	0.2423	1.2253E-05	7.0512E-06
	Micrococcales	N	Dark	Light	25	21	353	0.0754	0.0471	1.1898E-05	6.9638E-06
Methanogenesis	Methanocellales	N	Dark	Light	42	46	1059	0.44000	0.55000	1.6998E-05	1.5320E-05
	Methanocellales	Y	Dark	Light	40	87	2373	0.27500	0.39290	1.3283E-05	1.2860E-05
	Methanomassiliicoccales	N	Dark	Light	3	4	7	0.85700	0.85700	1.6954E-05	1.6526E-05
	Methanomassiliicoccales	Y	Dark	Light	2	6	5	0.85700	0.85700	8.6886E-06	9.6586E-06
	Methanomicrobiales	N	Dark	Light	120	129	8575	0.14200	0.23670	1.5618E-05	1.3928E-05
	Methanomicrobiales	Y	Dark	Light	130	202	20763	0.12300	0.23670	1.3696E-05	1.2621E-05
Chemotrophic	Anaerolineales	N	Dark	Light	22254	22254	247063666.0000	0.6140	0.7859	-9.2683	-9.4748
	Caldilineales	N	Dark	Light	48	48	1041.0000	0.1430	0.2542	-9.6052	-10.3627
	Caldilineales	Y	Dark	Light	48	48	1011.5000	0.1140	0.2146	-9.6477	-9.7787
	Cytophagales	N	Dark	Light	126	126	7879.0000	0.7530	0.8606	-10.3922	-11.3370
	Cytophagales	Y	Dark	Light	126	126	7383.0000	0.0275	0.0677	-10.5618	-11.0283
	Desulfobacterales	N	Dark	Light	114	114	6333.0000	0.5100	0.6800	-9.6052	-9.8249
	Desulfobacterales	Y	Dark	Light	114	114	5827.0000	0.0360	0.0823	-9.6118	-11.1583
	Flavobacteriales	N	Dark	Light	108	108	5993.0000	0.1800	0.3032	-11.4469	-10.1653
	Holophagales	N	Dark	Light	2058	2058	2104314.0000	0.2310	0.3696	-11.2496	-11.2639
	Methanomassiliicoccales	N	Dark	Light	12	12	67.0000	0.7460	0.8606	-10.1510	-10.1775
	Methanomassiliicoccales	Y	Dark	Light	12	12	47.0000	0.0919	0.1838	-10.8309	-10.7415
	Methanosarcinales	N	Dark	Light	2904	2904	4213844.0000	0.9460	0.9460	-10.2128	-10.4207
	Methylococcales	N	Dark	Light	912	912	414504.0000	0.8250	0.9103	-9.7091	-10.0295
	Micrococcales	N	Dark	Light	228	228	26538.5000	0.4580	0.6372	-10.5051	-11.0407
	Micrococcales	Y	Dark	Light	228	228	24450.0000	0.0565	0.1205	-10.5121	-11.1541
	Oscillospirales	N	Dark	Light	354	354	62450.0000	0.9000	0.9290	-9.8119	-10.2453
	Peptostreptococcales	N	Dark	Light	66	66	2213.0000	0.6860	0.8443	-11.2496	-11.6762
	Sphingomonadales	N	Dark	Light	948	948	453915.0000	0.4110	0.6263	-10.4202	-10.9573
	Verrucomicrobiales	Y	Dark	Light	648	648	208092.5000	0.4490	0.6372	-10.2687	-10.5036
	Vicinamibacterales	N	Dark	Light	564	564	159435.5000	0.9000	0.9290	-9.5197	-10.1166
	Vicinamibacterales	Y	Dark	Light	564	564	151716.0000	0.0231	0.0616	-9.4264	-10.4201

*Dark (Log Med.)" and "Light (Log Med.)" refer to the median log-transformed abundance of each category under dark and light conditions, respectively.

APPENDIX 7

Appendix 7. Comparison of median log-transformed functional category abundance between H-02 and Sarracenia Bay microcosms

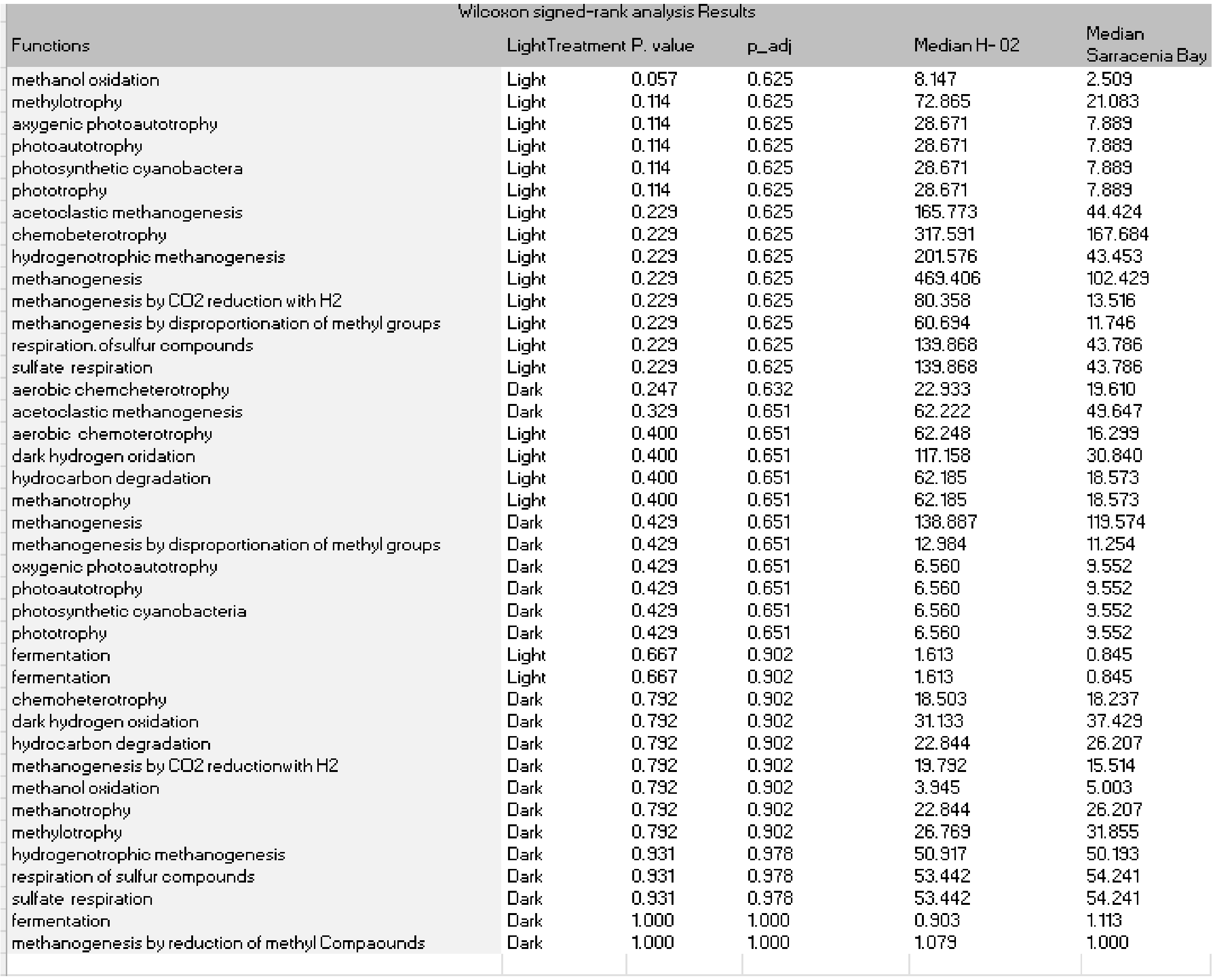

Wilcoxon signed-rank analysis Results

Functions	LightTreatment	P. value	p_adj	Median H- 02	Median Sarracenia Bay
methanol oxidation	Light	0.057	0.625	8.147	2.509
methylotrophy	Light	0.114	0.625	72.865	21.083
axygenic photoautotrophy	Light	0.114	0.625	28.671	7.889
photoautotrophy	Light	0.114	0.625	28.671	7.889
photosynthetic cyanobactera	Light	0.114	0.625	28.671	7.889
phototrophy	Light	0.114	0.625	28.671	7.889
acetoclastic methanogenesis	Light	0.229	0.625	165.773	44.424
chemobeterotrophy	Light	0.229	0.625	317.591	167.684
hydrogenotrophic methanogenesis	Light	0.229	0.625	201.576	43.453
methanogenesis	Light	0.229	0.625	469.406	102.429
methanogenesis by CO2 reduction with H2	Light	0.229	0.625	80.358	13.516
methanogenesis by disproportionation of methyl groups	Light	0.229	0.625	60.694	11.746
respiration.ofsulfur compounds	Light	0.229	0.625	139.868	43.786
sulfate respiration	Light	0.229	0.625	139.868	43.786
aerobic chemcheterotrophy	Dark	0.247	0.632	22.933	19.610
acetoclastic methanogenesis	Dark	0.329	0.651	62.222	49.647
aerobic chemoterotrophy	Light	0.400	0.651	62.248	16.299
dark hydrogen oridation	Light	0.400	0.651	117.158	30.840
hydrocarbon degradation	Light	0.400	0.651	62.185	18.573
methanotrophy	Light	0.400	0.651	62.185	18.573
methanogenesis	Dark	0.429	0.651	138.887	119.574
methanogenesis by disproportionation of methyl groups	Dark	0.429	0.651	12.984	11.254
oxygenic photoautotrophy	Dark	0.429	0.651	6.560	9.552
photoautotrophy	Dark	0.429	0.651	6.560	9.552
photosynthetic cyanobacteria	Dark	0.429	0.651	6.560	9.552
phototrophy	Dark	0.429	0.651	6.560	9.552
fermentation	Light	0.667	0.902	1.613	0.845
fermentation	Light	0.667	0.902	1.613	0.845
chemoheterotrophy	Dark	0.792	0.902	18.503	18.237
dark hydrogen oxidation	Dark	0.792	0.902	31.133	37.429
hydrocarbon degradation	Dark	0.792	0.902	22.844	26.207
methanogenesis by CO2 reductionwith H2	Dark	0.792	0.902	19.792	15.514
methanol oxidation	Dark	0.792	0.902	3.945	5.003
methanotrophy	Dark	0.792	0.902	22.844	26.207
methylotrophy	Dark	0.792	0.902	26.769	31.855
hydrogenotrophic methanogenesis	Dark	0.931	0.978	50.917	50.193
respiration of sulfur compounds	Dark	0.931	0.978	53.442	54.241
sulfate respiration	Dark	0.931	0.978	53.442	54.241
fermentation	Dark	1.000	1.000	0.903	1.113
methanogenesis by reduction of methyl Compaounds	Dark	1.000	1.000	1.079	1.000

*"Dark (Log Med.)" and "Light (Log Med.)" refer to the median log-transformed abundance of each category under dark and light conditions, respectively.

APPENDIX 8

Appendix 8. Non-significant comparisons of median log-transformed functional category abundance between light and dark treatments

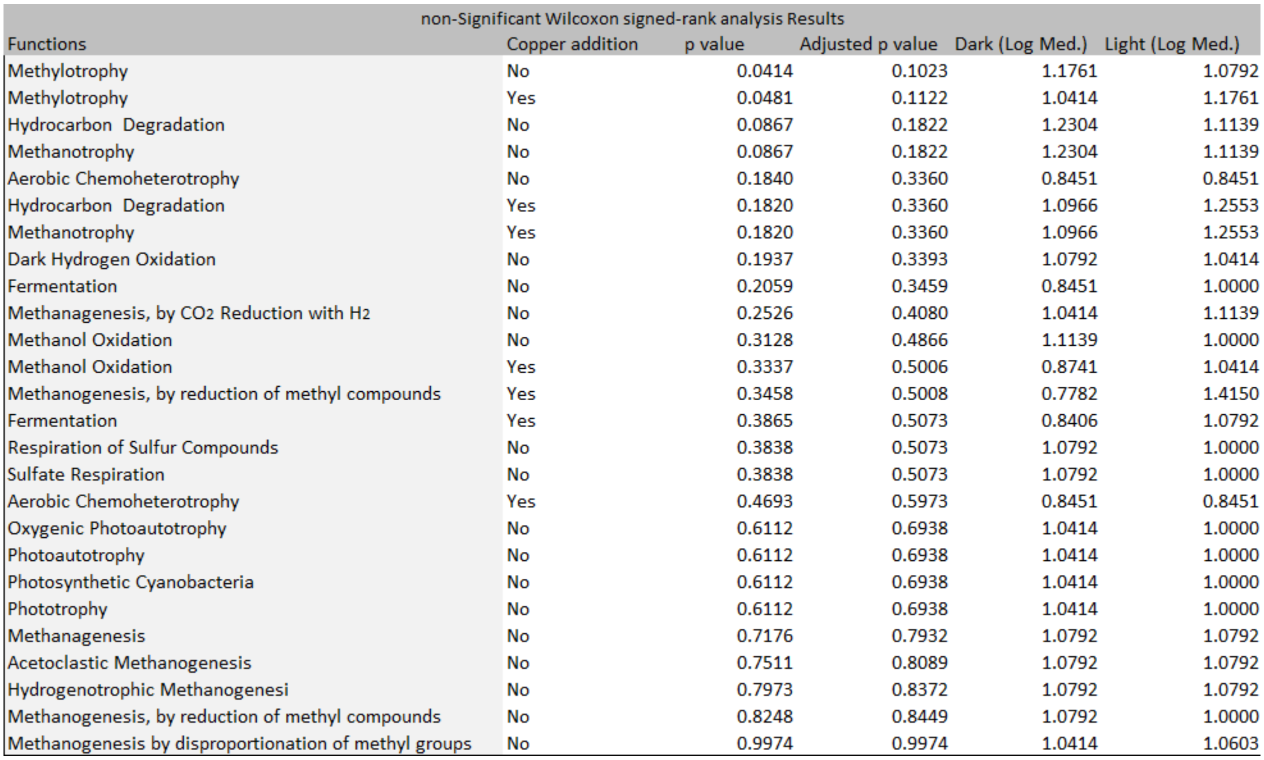

non-Significant Wilcoxon signed-rank analysis Results

Functions	Copper addition	p value	Adjusted p value	Dark (Log Med.)	Light (Log Med.)
Methylotrophy	No	0.0414	0.1023	1.1761	1.0792
Methylotrophy	Yes	0.0481	0.1122	1.0414	1.1761
Hydrocarbon Degradation	No	0.0867	0.1822	1.2304	1.1139
Methanotrophy	No	0.0867	0.1822	1.2304	1.1139
Aerobic Chemoheterotrophy	No	0.1840	0.3360	0.8451	0.8451
Hydrocarbon Degradation	Yes	0.1820	0.3360	1.0966	1.2553
Methanotrophy	Yes	0.1820	0.3360	1.0966	1.2553
Dark Hydrogen Oxidation	No	0.1937	0.3393	1.0792	1.0414
Fermentation	No	0.2059	0.3459	0.8451	1.0000
Methanagenesis, by CO_2 Reduction with H_2	No	0.2526	0.4080	1.0414	1.1139
Methanol Oxidation	No	0.3128	0.4866	1.1139	1.0000
Methanol Oxidation	Yes	0.3337	0.5006	0.8741	1.0414
Methanogenesis, by reduction of methyl compounds	Yes	0.3458	0.5008	0.7782	1.4150
Fermentation	Yes	0.3865	0.5073	0.8406	1.0792
Respiration of Sulfur Compounds	No	0.3838	0.5073	1.0792	1.0000
Sulfate Respiration	No	0.3838	0.5073	1.0792	1.0000
Aerobic Chemoheterotrophy	Yes	0.4693	0.5973	0.8451	0.8451
Oxygenic Photoautotrophy	No	0.6112	0.6938	1.0414	1.0000
Photoautotrophy	No	0.6112	0.6938	1.0414	1.0000
Photosynthetic Cyanobacteria	No	0.6112	0.6938	1.0414	1.0000
Phototrophy	No	0.6112	0.6938	1.0414	1.0000
Methanagenesis	No	0.7176	0.7932	1.0792	1.0792
Acetoclastic Methanogenesis	No	0.7511	0.8089	1.0792	1.0792
Hydrogenotrophic Methanogenesi	No	0.7973	0.8372	1.0792	1.0792
Methanogenesis, by reduction of methyl compounds	No	0.8248	0.8449	1.0792	1.0000
Methanogenesis by disproportionation of methyl groups	No	0.9974	0.9974	1.0414	1.0603

*Dark (Log Med.)" and "Light (Log Med.)" refer to the median log-transformed abundance of each category under dark and light conditions, respectively.

AUTHOR CONTRIBUTIONS SECTION

Co-author Dr Xiaoyu Xu contributed to refining the experimental design and provided critical edits to the manuscript.
Co-author Emma Kelsick contributed to statistical analysis and bioinformatic functional prediction of DNA sequence data.

All Co-authors agree that the work may be included in this thesis or dissertation.
Co-author Dr Xiaoyu Xu signature: Xiaoyu Xu
Co-author Emma Kelsick signature: Emma Kelsick

Due diligence was used to allow all co-authors an opportunity to respond.